A Multi-Configuration Mixing Approach with Symmetry-Projected Complex Hartree-Fock-Bogoliubov Determinants

E. Bender, K.W. Schmid and Amand Faessler

Institut für Theoretische Physik
Universität Tübingen
Auf der Morgenstelle 14
72076 Tübingen

Abstract

A multi-configuration mixing approach built on essentially complex, symmetry-projected Hartree-Fock-Bogoliubov (HFB) mean fields is introduced. The mean fields are obtained by variation after projection. The configuration space consists out of the symmetry-projected HFB vacuum and the symmetry-projected two-quasiparticle excitations for even, and the symmetry-projected one-quasiparticle excitations for odd A systems. The underlying complex HFB transformations are assumed to be time-reversal invariant and axially symmetric. The model allows nuclear structure calculations in large model spaces with arbitrary two-body interactions. The approach has been applied to ^{20}Ne and ^{22}Ne. Good agreement with the exact shell model results and considerable improvement with respect to older calculations, in which only real HFB transformations were admitted, is obtained.

1 Introduction

The shell model configuration mixing model ([1], [2], [3]) in general yields a very good description of at least the low energy phenomena in nuclear structure physics. Due to the large dimensions of the configuration spaces, however, complete shell model calculations are restricted to rather small basis systems, typically of the size of the $1s0d$ shell [4]. For the description of many nuclear structure problems one needs much larger basis systems. Examples are the investigation of giant resonances, medium-heavy and heavy nuclei and even comparatively simple tasks like the study of negative parity states in light even-even nuclei. In all these cases one is forced to truncate the complete shell model expansion of the nuclear wave functions to a manageable number of many nucleon configurations.

One way to achieve this is provided by the use of variational approaches, which leave the selection of the relevant configurations entirely to the dynamics of the system. The simplest models of this type are the well known Hartree-Fock ([5], [6]) and the more general Hartree-Fock-Bogoliubov (HFB) ([7], [8], [9], [10]) approaches. Though the nuclear ground state is approximated here by one single generalized Slater determinant only, this configuration usually accounts for a large part of the shell model expansion of the nuclear ground state. However, in general it breaks all the symmetries required by the many-nucleon Hamiltonian. Thus it cannot be considered as a physical state but only as some intrinsic structure, from which the physical components have still to be obtained with the help of projection techniques. Moreover, in order to obtain really optimal solutions for each set of simultaneously conserved quantum numbers separately, the restoration of the broken symmetries has to be performed before the mean field is determined by the variation.

A whole hierarchy of such symmetry-conserving variational approaches on the basis of HFB-type configurations have been proposed by some of us a couple of years ago [11]. They have become known as the VAMPIR (**V**ariation **A**fter **M**ean field **P**rojection **I**n **R**ealistic model spaces) and the MONSTER (**MO**del for handling many **N**umber- and **S**pin-projected **T**wo-quasiparticle **E**xcitations with **R**ealistic interactions and model spaces) approaches.

In the VAMPIR model ([12], [13]) the energetically lowest state of a particular spin-parity is approximated by a single symmetry-projected HFB vacuum and the underlying HFB transformation is determined by variation after the projection onto the desired quantum numbers. Excited states with the same quantum numbers can be obtained by repeating this procedure with a new HFB test vacuum which is constrained to be orthogonal to all the solutions already obtained. Finally then, in this EXCITED VAMPIR model ([13], [14]) the residual interaction between all the obtained solutions is diagonalized. A straightforward extension of these approaches are

the Few Determinant (FED) VAMPIR and the EXCITED FED VAMPIR models ([15], [16]), which approximate each state not by a single, but by a linear combination of several non-orthogonal symmetry-projected HFB configurations, which are again determined by independent, successive variations. By such chains of variational calculations the lowest few states of a given symmetry representation can be obtained, irrespective of their particular structure.

The methods are bound to fail, however, if the complete excitation spectrum with respect to a particular transition operator is to be described, like e.g., in the description of giant multipole resonances. If this transition operator is of one body nature, it is obviously preferable to consider only excited states with a similar structure like the corresponding ground (or yrast) state. One way to achieve this is to expand the nuclear wave function around a symmetry projected reference vacuum, which may either be the usual HFB or, e.g., a VAMPIR solution. This is the essence of the MONSTER approach ([11], [17], [4]), in which the residual interaction is diagonalized in the space of the symmetry-projected vacuum and all the two-quasiparticle excitations with respect to it, if an even system is considered while for odd systems the configuration space is limited to the symmetry-projected one-quasiparticle configurations.

Unfortunately, in all applications up to now, these models had to be simplified out of numerical reasons. This was achieved by imposing certain symmetry restrictions on the underlying HFB transformations. Consequently, the corresponding HFB vacua do not contain all principally possible correlations, but only a particular part of them, which becomes more and more restricted as more symmetry requirements are imposed.

In the first VAMPIR calculations only real, time-reversal invariant and axially symmetric HFB transformations, which neither mix proton and neutron states nor states of different parity, were admitted [12]. With this *real* VAMPIR approach, as such calculations are called in the following, only states in even-even nuclei with even spin and positive parity could be described. If a MONSTER calculation is based on such a *real* VAMPIR transformation, the states with different symmetries (e.g., odd spins) are introduced by the configuration mixing. However, odd spin, or negative parity states in the same even-even nucleus, or states in a neighbouring odd-odd nucleus may have a structure, which differs considerably from the structure of the real reference vacuum. Thus they cannot neccessarily be described well with the *real* MONSTER on VAMPIR approach.

A few years ago then the VAMPIR approach has been improved ([13], [18]) by allowing essentially complex HFB transformations as well as parity- and proton-neutron-mixing. Only time-reversal and axial symmetry were kept. In this *complex* VAMPIR approach many more nucleon correlations are considered and states of

arbitrary spin parity in even mass nuclei can be described.

In the present work for the first time MONSTER calculations on the basis of such more general *complex* VAMPIR transformations are performed. The corresponding configuration spaces are considerably larger than those of the older, more restricted real calculations and consequently a much better description of many states is expected. Furthermore, now also the calculations for odd-odd nuclei can be based on transformations particularly derived for such systems, and only for the description of odd systems one has still to rely on mean fields obtained for neighbouring nuclei as in the older approach. However, even here the underlying transformations are more general and consequently the configuration spaces much larger than earlier and thus more correlations can be described.

In the next section (2.1) we summarize the essential features of the VAMPIR approach without any symmetry restrictions. We then proceed in section (2.2) by outlining the general formalism for MONSTER calculations on the basis of the corresponding VAMPIR solutions. In section (2.3) then the consequences of various symmetry restrictions on the underlying HFB transformation are discussed and explicit formulas for the MONSTER approach restricted to essentially complex, but still time-reversal invariant and axially symmetric HFB transformations are derived. As a first test this method is applied to the two nuclei ^{20}Ne and ^{22}Ne. Here only a small single particle basis, the $1s0d$-shell was considered. This allows to compare the results not only to those of the more restricted *real* MONSTER approach but also with complete shell model diagonalizations. This is done in section (3). Finally, in section (4) the present work is summarized.

2 Theory

2.1 The VAMPIR model

The model space is defined by a finite, D-dimensional set of orthonormal single particle states $\mathcal{D} = \{|i\rangle, |k\rangle, \ldots\}_D$. The indices i, k are standing for the set of quantum numbers characterizing the state. The corresponding creation and annihilation operators are denoted by $\{c_i^\dagger, c_k^\dagger, \ldots\}_D$ and $\{c_i, c_k, \ldots\}_D$, respectively. They obey the anti-commutation relations for Fermion operators. We assume that the effective many-body Hamiltonian appropriate for the chosen model space is known and can be represented by a sum of only one- and two-body terms

$$\hat{H} = \sum_{ik} t(ik) c_i^\dagger c_k + \frac{1}{4} \sum_{ikrs} v(ikrs) c_i^\dagger c_k^\dagger c_s c_r, \tag{1}$$

where $t(ik) = \langle i|\hat{t}|k\rangle$ are the one-body matrix elements of the kinetic energy (or some single particle energies) while $v(ikrs) = \langle ik|\hat{v}|rs - sr\rangle$ denote the anti-symmetrized two-body matrix elements of the effective interaction.

We then introduce quasiparticle creation- and annihilation operators $a^\dagger$ and a via the Hartree-Fock-Bogoliubov transformation [10] which in matrix notation is given by

$$\begin{pmatrix} a^\dagger(F) \\ a(F) \end{pmatrix} = F \begin{pmatrix} c^\dagger \\ c \end{pmatrix} = \begin{pmatrix} A^T(F) & B^T(F) \\ B^+(F) & A^+(F) \end{pmatrix} \begin{pmatrix} c^\dagger \\ c \end{pmatrix}. \tag{2}$$

This is the most general linear transformation conserving the Fermion anti-commutation relations, provided the transformation matrix F is chosen to be unitary. Via the inverse transformation the Hamiltonian (1) can be represented in terms of the quasiparticle creation and annihilation operators as

$$\hat{H} = H^0(F) + \hat{H}^{11}(F) + \hat{H}^{20}(F) + \hat{H}^{22}(F) + \hat{H}^{31}(F) + \hat{H}^{40}(F), \tag{3}$$

with the upper indices denoting the number of creators and annihilators (or vice versa), respectively. Explicit expressions for the various terms can be found in [11]. The vacuum for quasiparticle annihilators is given by [19]

$$|F\rangle = \left(\prod_{\alpha=1}^{D'} a_\alpha(F) \right) |0\rangle. \tag{4}$$

Here $|0\rangle$ is the particle vacuum and α enumerates the quasiparticle states. The product runs over all quasiparticle annihilation operators with $a_\alpha(F)|0\rangle \neq 0$. Since the HFB transformation generally mixes basis states of all different quantum numbers, the vacuum is neither an eigenstate of the square of the angular momentum operator, nor of its z-component. Furthermore it has neither good proton nor good neutron number. The only symmetry which is still conserved is the so called number parity [19], i.e. the vacuum contains either only even or only odd nucleon number components. n-quasiparticle states with respect to this vacuum $|F\rangle$ can then be defined by

$$|F\{a^\dagger\}_n\rangle = \begin{cases} |F\rangle & \text{for} \quad n = 0 \\ \left(\prod_{\alpha=1}^{n} a_\alpha^\dagger(F) \right) |F\rangle & \text{for} \quad n = 1, \ldots, D. \end{cases} \tag{5}$$

Obviously, the n-quasiparticle states, too, do violate the above mentioned symmetries. In order to obtain physical states, these have to be restored before in a particular selection of such configurations the energetically deepest solutions are determined by variation. Since any of the n-quasiparticle configurations can be written as vacuum to a particular set of quasiparticle annihilators, only HFB vacua will be discussed in the rest of this section.

The restoration of the broken symmetries is achieved with the help of projection operators ([11], [13]). Good parity π is, e.g., restored by the operator

$$\hat{P}(\pi) = \frac{1}{2}\left[1 + \pi\hat{\Pi}\right]. \tag{6}$$

The restoration of good proton and neutron number is equivalent to projecting the nuclear wave function on a good mass number A and good T_z-component of isospin. The corresponding operators are is given by

$$\hat{P}(A) = \frac{1}{2\pi}\int_0^{2\pi} d\phi\, e^{i\phi A}\hat{S}_A(\phi) \quad \text{where} \quad \hat{S}_A(\phi) \equiv e^{-i\phi\hat{A}}, \tag{7}$$

and

$$\hat{P}(2T_z) = \frac{1}{2\pi}\int_0^{2\pi} d\chi\, e^{i\chi 2T_z}\hat{S}_{2T_z}(\chi) \quad \text{where} \quad \hat{S}_{2T_z}(\chi) \equiv e^{-i\chi 2\hat{T}_z}, \tag{8}$$

respectively. The desired angular momentum quantum numbers can be obtained by an integral operator, too. It is given by

$$\hat{P}(IM;K) = \frac{2I+1}{8\pi^2}\int d\Omega\, D^{I*}_{MK}(\Omega)\hat{R}(\Omega) \tag{9}$$

where $\hat{R}(\Omega)$ is the usual rotation operator and $D^I_{MK}(\Omega)$ its representation in angular momentum eigenstates. The integration is running over the full three Euler angles. These projection operators commute with each other and with the Hamiltonian. In shorthand notation we define

$$\hat{\Theta}^{AT_zI^\pi}_{MK} \equiv \hat{P}(IM;K)\hat{P}(2T_z)\hat{P}(A)\hat{P}(\pi). \tag{10}$$

Physical configurations with good symmetry S, where S represents the quantum numbers AT_zI^π, are then obtained applying the projector $\hat{\Theta}^S_{MK}$ on the above quasiparticle configurations. For any quasiparticle vacuum $|F\rangle$, e.g., we obtain

$$|F;SM\rangle = \sum_{K=-I}^{I}\hat{\Theta}^S_{MK}|F\rangle f^S_K. \tag{11}$$

Note that one has to take the sum over all angular momentum z-components K. Otherwise the projected wave function would depend on the orientation of the intrinsic reference frame [11].

The VAMPIR approach restricts the configuration space for the lowest (the "yrast") state of a given symmetry S to such a single symmetry projected vacuum. The

configuration mixing degrees of freedom f_K^S as well as the underlying HFB transformation F are then determined by variation

$$\delta E^S \equiv \delta \frac{\langle F; SM|\hat{H}|F; SM\rangle}{\langle F; SM|F; SM\rangle} = 0. \tag{12}$$

Performing this variation one obtains the optimal description of the considered yrast state by only a single determinant.

The variation leads to three sets of equations which have to be solved self-consistently. The first set, resulting from the variation with respect to the mixing degrees of freedom f_K^S in (11), is the diagonalization of the Hamiltonian (1) in the space of the non-orthogonal configurations $\hat{\Theta}^S_{MK}|F\rangle$

$$\sum_{K'=-I}^{I} \left\{ H^S_{KK'} - E^S N^S_{KK'} \right\} f^S_{K'} = 0 \tag{13}$$

with the constraint

$$(f^S)^+ N^S f^S = \mathbf{1} \tag{14}$$

which ensures the orthonormality of the resulting states. The Hamiltonian and the overlap matrices in these equations are given by

$$\begin{aligned} H^S_{KK'} &= \langle F; SMK|\hat{H}|F; SMK'\rangle \\ N^S_{KK'} &= \langle F; SMK|F; SMK'\rangle \end{aligned} \qquad \text{where} \quad |F; SMK\rangle \equiv \hat{\Theta}^S_{MK}|F\rangle. \tag{15}$$

The variation with respect to the HFB transformation leads to the second set of equations. An elegant way to perform this variation is provided by Thouless's Theorem [20]. It states that any HFB vacuum $|F^d\rangle$ can be represented in terms of an arbitrarily chosen reference vacuum $|F^0\rangle$, non-orthogonal to $|F^d\rangle$, as

$$|F^d\rangle = \langle F^0|F^d\rangle \exp\left\{ \frac{1}{2} \sum_{\mu\nu} d_{\mu\nu} a^\dagger_\mu(F^0) a^\dagger_\nu(F^0) \right\} |F^0\rangle, \tag{16}$$

with d being an anti-symmetric $D \times D$ matrix. The quasiparticles which belong to the vacuum $|F^d\rangle$ are related to those of the vacuum $|F^0\rangle$ via

$$\begin{aligned} \begin{pmatrix} a^\dagger(F^d) \\ a(F^d) \end{pmatrix} &= \begin{pmatrix} L_d^{-1*} & -(L_d^{-1}d)^* \\ -L_d^{-1}d & L_d^{-1} \end{pmatrix} \begin{pmatrix} a^\dagger(F^0) \\ a(F^0) \end{pmatrix} \\ &\text{with} \quad \mathbf{1} + d^T d^* = L_d L_d^+. \end{aligned} \tag{17}$$

Consequently the variation with respect to the matrix elements of F can be replaced by the variation with respect to the matrix elements of d. One obtains

$$\frac{\partial E^S}{\partial d_{\alpha\beta}} = \sum_{\gamma\delta} \left(L_d^{-1}\right)^T_{\alpha\gamma} \tilde{g}_{\gamma\delta} \left(L_d^{-1}\right)_{\delta\beta} = 0$$

$$\text{where} \quad \tilde{g}_{\gamma\delta} \equiv \sum_{KK'} f^{S*}_K \langle F^d | [\hat{H} - E^S] \hat{\Theta}^S_{KK'} a^\dagger_\gamma(F^d) a^\dagger_\delta(F^d) | F^d \rangle f^S_{K'}. \tag{18}$$

This equation (a sort of generalized Brillouin theorem) expresses the stability of the solution (11) against arbitrary projected two-quasiparticle states with the same symmetry S.

Since the HFB vacuum is invariant under unitary transformation of the quasiparticle operators among themselves, these two sets of equations are not yet sufficient to determine the HFB transformation unambiguously. As usual we use this freedom to diagonalize the one-quasiparticle spectrum. This yields a third set of equations

$$\langle F | a_\alpha(F) \hat{H} a^\dagger_\beta(F) | F \rangle - \delta(\alpha,\beta) \langle F | \hat{H} | F \rangle = E_\alpha \, \delta(\alpha,\beta). \tag{19}$$

The eigenvalues E_α are called quasiparticle energies.

These three sets form the VAMPIR variational equations [13]. Their solution yields in general already a rather good description for the yrast states. If necessary, correlating symmetry projected configurations can be obtained by successive variational calculations. This is done in the FED VAMPIR approach [15]. Furthermore, using orthonormality contraints, the procedure can be easily extended to the description of excited states. This is done in the EXCITED VAMPIR [13], and the even more general EXCITED FED VAMPIR [15] approaches. In principle, with the help of these approaches nuclear states of arbitrary complexity can be described. However, these methods are specifically designed, to obtain wave functions for the lowest few states of a given symmetry S only. They can hardly be applied if, e.g., the complete excitation spectrum with respect to some (usually one-body) transition operator is required. For such problems it is preferable to consider only specific configurations as they can be obtained by expanding the nuclear wave functions around a suitable VAMPIR vacuum. This is demonstrated in the following section.

2.2 The MONSTER on VAMPIR approach

For a particular symmetry S we define a configuration space

$$\{|Q; SMK\rangle\} \equiv \{|F; SMK\rangle, \, |F\alpha\beta; SMK\rangle; \; \alpha < \beta; \; K = -I, \ldots, +I\} \tag{20}$$

consisting out of the symmetry-projected vacuum (see also (11))

$$|F;SMK\rangle \equiv \hat{\Theta}^S_{MK}|F\rangle \tag{21}$$

and the symmetry-projected two-quasiparticle states

$$|F\alpha\beta;SMK\rangle \equiv \hat{\Theta}^S_{MK}a^\dagger_\alpha(F)a^\dagger_\beta(F)|F\rangle \tag{22}$$

with respect to it. Note that S needs not necessarily be identical to the symmetry for which the underlying VAMPIR mean field is obtained. In many cases it will be sufficient to use just the VAMPIR transformation obtained for the ground state of the considered system.

The above choice of the configuration space ensures that the total wave functions of the excited states being linear combinations of these (non orthogonal) configurations

$$\begin{aligned} |\psi_i(F);SM\rangle &= \left\{\sum_K |F;SMK\rangle g^S_{0K;i} + \sum_{\alpha<\beta,K} |F\alpha\beta;SMK\rangle g^S_{\alpha\beta K;i}\right\} \\ &= \sum_Q |Q;SMK\rangle g^S_{QK;i} \end{aligned} \tag{23}$$

are similar in structure as the projected vacuum and can hence easily be reached from the latter by, e.g., one-body transition operators. The configuration mixing degrees of freedom $g^S_{QK;i}$ can then be obtained by diagonalizing the Hamiltonian matrix (1)

$$\sum_{Q'}\left\{H^S_{QK;Q'K'} - E^S N^S_{QK;Q'K'}\right\} g^S_{Q'K'} = 0 \tag{24}$$

being subject to the usual orthonormality constraint

$$(g^S)^+ N^S g^S = \mathbf{1}. \tag{25}$$

Note that the sum over Q in (23) and (24) includes implicitly the sum over the K-components. The Hamiltonian and overlap matrix elements entering the above equations are given by

$$\begin{aligned} H^S_{QK;Q'K'} &= \langle Q;SMK|\hat{H}\hat{\Theta}^S_{KK'}|Q';SMK'\rangle \\ N^S_{QK;Q'K'} &= \langle Q;SMK|\hat{\Theta}^S_{KK'}|Q';SMK'\rangle. \end{aligned} \tag{26}$$

As all shell model approaches, the above diagonalization (24,25) yields many-nucleon wave functions which are contaminated by spurious center-of-mass (CM) excitations [21], if the single particle basis $\mathcal{D}$ contains more than one major oscillator shell. In the MONSTER on VAMPIR approach these spurious admixtures are eliminated at least approximately by a method originally proposed by Giraud [22], which is

based on the following argument. For a pure harmonic oscillator basis an exact separation of the *CM* motion is possible if all oscillator many-particle determinants with energies up to a certain $n\hbar\omega$ are included in the configuration space. The *CM* Hamiltonian is given in that case by

$$\hat{H}^{CM} = \hat{T}^{CM} + \hat{V}^{CM} = \frac{\hat{\mathbf{P}}^2}{2Am} + \frac{1}{2}Am\omega^2\mathbf{R}^2 \tag{27}$$

with $\mathbf{R} = (1/A)\sum_{i=1}^{A}\mathbf{r}_i$ and $\hat{\mathbf{P}} = \sum_{i=1}^{A}\hat{\mathbf{p}}_i$, where $\mathbf{r}_i$ are the spatial coordinates and $\hat{\mathbf{p}}_i$ the momentum operators of the particles $i = 1, \ldots, A$. ω is the harmonic oscillator constant and m the nucleon mass. After diagonalizing the *CM* Hamiltonian in the $n\hbar\omega$ space, one can identify [21] the spurious *CM* components as $1\hbar\omega$, $2\hbar\omega$, ..., $n\hbar\omega$ excitations and can eliminate them. For any other basis it is not possible to choose a model space which is complete with respect to $n\hbar\omega$ oscillator excitations. However, the diagonalization of the *CM* Hamiltonian will produce energy eigenvalues which are still clustered around the exact excitation energies [23]. By eliminating the corresponding eigenstates at least the predominant spurious components are removed. Therefore instead of solving equations (24,25), we first diagonalize the *CM* Hamiltonian $\hat{H}^{CM}$ in the chosen non-orthogonal basis (20)

$$\sum_{Q'}\left\{H^{CM;S}_{QK;Q'K'} - E^{CM;S}N^{S}_{QK;Q'K'}\right\}f^{S}_{Q'K'} = 0 \tag{28}$$

with the constraint

$$(f^S)^{+}N^S f^S = \mathbf{1}. \tag{29}$$

The solutions with excitation energies around $1\hbar\omega$, $2\hbar\omega$, ... are considered as spurious. Out of those, denoted by $|f_s\rangle$ $(s = 1, \ldots, n_s)$, we can construct a projection operator

$$\hat{P}_s = \mathbf{1} - \sum_{s=1}^{n_s}|f_s\rangle\langle f_s|, \tag{30}$$

which modifies the effective Hamiltonian (1) into

$$\hat{\tilde{H}} = \hat{P}_s\hat{H}\hat{P}_s. \tag{31}$$

The diagonalization problem (24,25) is then solved for the modified instead of the original Hamiltonian. The spurious states occur now at energies $E^S \sim 0$ and can hence be easily identified.

2.3 Restriction to complex time-reversal invariant and axially symmetric HFB transformations

If no symmetry restrictions are imposed on the HFB transformations, symmetry-projected vacua of the type (11) can be used to describe arbitrary states in arbitrary

nuclei [13]. This, however, has not been achieved up to now out of numerical reasons. Instead, for the existing numerical realisations of the VAMPIR approaches, certain symmetry requirements were imposed on the underlying HFB transformations.

So, e.g., in the first VAMPIR calculations [12], axial symmetry and time-reversal invariance were required, parity- and proton-neutron mixing were neglected and only real HFB transformations were admitted. Consequently such *real* VAMPIR solutions were only suitable for even spin, positive parity states in doubly even nuclei. Performing MONSTER calculations on top of such solutions, obviously these restrictions are removed and states with arbitrary spin-parity in doubly even, doubly odd and (in one-quasiparticle approximation) odd systems become accessible, too. However, for their calculation one has to rely on mean fields obtained for different spin values than the considered one and, for doubly odd and odd mass systems even for neighbouring nuclei.

In the more recent implementations of the VAMPIR approaches then parity- as well as proton-neutron mixing were taken into account and essentially complex HFB transformations were admitted. This introduces many more correlations into the projected vacua as in the older calculations and furthermore makes states with arbitrary spin and parity in both doubly even and doubly odd nuclei accessible. In these *complex* VAMPIR approaches only axial symmetry and time-reversal invariance are kept. Thus the quasiparticle spectrum is still twofold degenerate and hence only states in even mass nuclei can be described [13]. The MONSTER approach, however, was up to now still limited to the use of *real* VAMPIR solutions. In the present work for the first time *complex* VAMPIR solutions have been used in such multi-configuration mixing calculations.

The mathematical apparatus of the *complex* VAMPIR approach has been described in detail elsewhere [13]. In the following we shall therefore only scetch the essential ingredients and concentrate on those features which are needed in a subsequent MONSTER type calculation.

Time-reversal invariance is imposed on the HFB transformation by requiring that with any creator $a^\dagger_\alpha$ also its time-reversed partner $a^\dagger_{\bar{\alpha}} = \hat{\tau} a^\dagger_\alpha \hat{\tau}^{-1}$, where $\hat{\tau}$ is the time-reversal operator, belongs to the same quasiparticle representation. Axial symmetry is enforced by conserving the z-component of the angular momentum. For the transformation coefficients of the HFB transformation (2) we get in this case the symmetries

$$\begin{aligned} A_{i\alpha}(F) &= \delta(m_i, m_\alpha) A_{i\alpha}(F) = \delta(m_i, m_\alpha) A^*_{\bar{i}\bar{\alpha}}(F), \\ B_{i\bar{\alpha}}(F) &= \delta(m_i, m_\alpha) B_{i\bar{\alpha}}(F) = -\delta(m_i, m_\alpha) B^*_{\bar{i}\alpha}(F), \\ A_{i\bar{\alpha}}(F) &= 0 \quad \text{and} \quad B_{i\alpha}(F) = 0. \end{aligned} \tag{32}$$

Because of these symmetries, the vacuum (11) becomes time-reversal invariant and furthermore an eigenstate of the z-component of total angular momentum with eigenvalue zero. Consequently also all the n-quasiparticle configurations (5) have a definite angular momentum z-projection.

These assumptions simplify the projection operator (10) considerably. Now two of the five integrations can be performed analytically and we obtain [13]

$$\begin{aligned}\hat{\Theta}^S_{KK'} &= \frac{2I+1}{2}\int_0^\pi d\vartheta \sin(\vartheta) d^I_{KK'}(\vartheta)\hat{R}(\vartheta)\frac{1}{(2\pi)^2}\int_{-\pi}^{\pi} d\varphi \int_0^\pi d\chi \\ &\quad \Big[w(\varphi,\chi)\hat{S}(\varphi,\chi) + w^*(\varphi,\chi)\hat{S}^*(\varphi,\chi)\Big]\frac{1}{2}\Big[1+\pi_S\hat{\Pi}\Big] \end{aligned} \tag{33}$$

with $\hat{R}(\vartheta) = \exp(-i\vartheta\hat{J}_y)$ and the definitions

$$\begin{aligned} w(\varphi,\chi) &\equiv \exp\Big\{i\Big[\tfrac{\varphi}{2}A + \tfrac{\chi}{2}(2T_z)\Big]\Big\}, \\ \hat{S}(\varphi,\chi) &\equiv \exp\Big\{-i\Big[\tfrac{\varphi}{2}\hat{A} + \tfrac{\chi}{2}(2\hat{T}_z)\Big]\Big\}. \end{aligned} \tag{34}$$

The VAMPIR variational equations (12) consisting of equations (13, 18 and 19) are also simplified considerably. The diagonalization (13) becomes now redundant since the vacuum has only one fixed angular momentum z-component $K = 0$. Explicit formulas for the *complex* VAMPIR variational equations can be found in [13]. Here we only want to mention that the *complex* VAMPIR vacuum contains still all possible two nucleon couplings. However, it does not contain all possible four- and more-nucleon couplings ([15], [18]). This becomes clear from the basic building blocks of the vacuum [13] : a natural parity four nucleon state is always built either by two natural parity or two unnatural parity pairs, but never by one natural parity and one unnatural parity pair. One natural parity pair and one unnatural parity pair always yield an unnatural four nucleon state. Analogously one can find the missing couplings for larger numbers of nucleons. States dominated by such couplings cannot be described well with the *complex* VAMPIR approach. To solve the *complex* VAMPIR variational equations one has to calculate Hamiltonian and overlap matrix elements in between the projected vacuum. They are also needed in the *complex* MONSTER approach and therefore shown here, although similar expressions can be found already in [13]. For convenience we introduce the abbreviations

$$\begin{aligned} |F_\lambda\rangle \equiv \begin{cases} |F\rangle \\ \hat{\Pi}|F\rangle \end{cases} \quad \text{and} \quad a^\dagger(F_\lambda) \equiv \begin{cases} a^\dagger(F) & \text{for } \lambda = 1 \\ \hat{\Pi}\, a^\dagger(F)\, \hat{\Pi}^{-1} & \text{for } \lambda = 2 \end{cases} \\ \hat{\tilde{R}}(\tilde{\Omega}) \equiv \hat{\tilde{R}}(\vartheta,\varphi,\chi) \equiv \hat{R}(\vartheta)\hat{S}(\varphi,\chi). \end{aligned} \tag{35}$$

The projected overlap matrix element in between two vacua, which belong to two different HFB transformations F^1 and F^2, is then given by

$$\begin{aligned}\langle F^1|\hat{\Theta}^S_{00}|F^2\rangle &= \frac{2I+1}{2}\int_0^\pi d\vartheta \sin(\vartheta) d^I_{00}(\vartheta)\frac{1}{(2\pi)^2}\int_{-\pi}^{\pi} d\varphi \int_0^\pi d\chi \\ &\Big\{\Re e\left[w(\varphi,\chi)\Big(n_1^{12}(\vartheta,\varphi,\chi)+\pi_S n_2^{12}(\vartheta,\varphi,\chi)\Big)\right]\Big\}, \end{aligned} \tag{36}$$

where the rotated overlap has been defined as

$$n^{12}_\lambda(\tilde{\Omega}) \equiv \langle F^1|\hat{\tilde{R}}(\tilde{\Omega})|F^2_\lambda\rangle. \tag{37}$$

$n^{12}_\lambda(\tilde{\Omega})$ is calculated as described in ([13], [24], [25]). General matrix elements in between two projected quasiparticle states can then be evaluated using a generalized version of Wick's Theorem. The only four non-vanishing elementary contractions are here

$$\langle F^1|a_\alpha(F^1)a^\dagger_\beta(F^1)\hat{\tilde{R}}(\tilde{\Omega})|F^2_\lambda\rangle \equiv \delta(\alpha,\beta)n^{12}_\lambda(\tilde{\Omega}), \tag{38}$$

$$\langle F^1|a_\beta(F^1)a_\alpha(F^1)\hat{\tilde{R}}(\tilde{\Omega})|F^2_\lambda\rangle \equiv [g^{12}_\lambda(\tilde{\Omega})]_{\alpha\beta}n^{12}_\lambda(\tilde{\Omega}), \tag{39}$$

$$\langle F^1|a_\alpha(F^1)\hat{\tilde{R}}(\tilde{\Omega})a^\dagger_\beta(F^2_\lambda)|F^2_\lambda\rangle \equiv [X^{12}_\lambda(\tilde{\Omega})]_{\alpha\beta}n^{12}_\lambda(\tilde{\Omega}), \tag{40}$$

$$\langle F^1|\hat{\tilde{R}}(\tilde{\Omega})a^\dagger_\alpha(F^2_\lambda)a^\dagger_\beta(F^2_\lambda)|F^2_\lambda\rangle \equiv [\tilde{g}^{12}_\lambda(\tilde{\Omega})]_{\alpha\beta}n^{12}_\lambda(\tilde{\Omega}), \tag{41}$$

where

$$X^{12}_\lambda(\tilde{\Omega}) \equiv [A^+_\lambda(F^1F^2;\tilde{\Omega})]^{-1}, \tag{42}$$

$$g^{12}_\lambda(\tilde{\Omega}) \equiv B^*_\lambda(F^1F^2;\tilde{\Omega})X^{12^T}_\lambda(\tilde{\Omega}), \tag{43}$$

$$\tilde{g}^{12}_\lambda(\tilde{\Omega}) \equiv B^T_\lambda(F^1F^2;\tilde{\Omega})X^{12}_\lambda(\tilde{\Omega}), \tag{44}$$

and the rotated transformation matrices are defined as

$$A_\lambda(F^1F^2;\tilde{\Omega}) \equiv A^+(F^1)\tilde{R}(\tilde{\Omega})A(F^2_\lambda) + B^+(F^1)\tilde{R}^*(\tilde{\Omega})B(F^2_\lambda), \tag{45}$$

$$B_\lambda(F^1F^2;\tilde{\Omega}) \equiv B^T(F^1)\tilde{R}(\tilde{\Omega})A(F^2_\lambda) + A^T(F^1)\tilde{R}^*(\tilde{\Omega})B(F^2_\lambda). \tag{46}$$

Here $A(F^i_\lambda)$ and $B(F^i_\lambda)$ are for $\lambda = 1$ just the HFB transformation matrices of the transformation F^i; in the case $\lambda = 2$ these coefficients are multiplied with the parity of the basis states. $\tilde{R}$ denotes the representation of $\hat{\tilde{R}}$ in the chosen single particle basis $\mathcal{D}$. Similarly the rotated energy function

$$h^{n^{12}}_\lambda(\tilde{\Omega}) \equiv \langle F^1|\hat{H}\hat{\tilde{R}}(\tilde{\Omega})|F^2_\lambda\rangle, \tag{47}$$

which is necessary for the calculation of the projected energy matrix element

$$\begin{aligned}\langle F^1|\hat{H}\hat{\Theta}^S_{00}|F^2\rangle &= \frac{2I+1}{2}\int_0^\pi d\vartheta \sin(\vartheta) d^I_{00}(\vartheta)\frac{1}{(2\pi)^2}\int_{-\pi}^{\pi} d\varphi \int_0^\pi d\chi \\ &\Big\{\Re e\left[w(\varphi,\chi)\Big(h_1^{n^{12}}(\vartheta,\varphi,\chi)+\pi_S h_2^{n^{12}}(\vartheta,\varphi,\chi)\Big)\right]\Big\} \end{aligned} \tag{48}$$

is obtained as

$$h_\lambda^{n^{12}}(\tilde{\Omega}) = h_\lambda^{12}(\tilde{\Omega}) n_\lambda^{12}(\tilde{\Omega}), \tag{49}$$

with

$$h_\lambda^{12}(\tilde{\Omega}) \equiv H^0(F^1) + \tilde{H}_\lambda^{20*}(F^1F^2;\tilde{\Omega}) + 3\tilde{\tilde{H}}_\lambda^{40*}(F^1F^2;\tilde{\Omega}), \tag{50}$$

and

$$\tilde{H}_\lambda^{20*}(F^1F^2;\tilde{\Omega}) \equiv \sum_{\alpha\beta} H_{\alpha\beta}^{20^*}(F^1)[g_\lambda^{12}(\tilde{\Omega})]_{\alpha\beta}, \tag{51}$$

$$\tilde{\tilde{H}}_\lambda^{40*}(F^1F^2;\tilde{\Omega}) \equiv \sum_{\alpha\beta} [\tilde{H}_\lambda^{40*}(F^1F^2;\tilde{\Omega})]_{\alpha\beta}[g_\lambda^{12}(\tilde{\Omega})]_{\alpha\beta}, \tag{52}$$

$$[\tilde{H}_\lambda^{40*}(F^1F^2;\tilde{\Omega})]_{\alpha\beta} \equiv \sum_{\gamma\delta} H_{\alpha\beta\gamma\delta}^{40^*}(F^1)[g_\lambda^{12}(\tilde{\Omega})]_{\gamma\delta}, \tag{53}$$

where H^0, H^{20} and H^{40} are Hamiltonian matrix elements of (3) in the quasiparticle representation.

In case of time-reversal invariance and axial symmetry the two-quasiparticle configurations can be written as

$$\begin{aligned}
&|F\alpha\beta\rangle \equiv a_\alpha^\dagger(F)a_\beta^\dagger(F)|F\rangle, \qquad |F\bar{\alpha}\bar{\beta}\rangle \equiv \hat{\tau}|F\alpha\beta\rangle = a_{\bar{\alpha}}^\dagger(F)a_{\bar{\beta}}^\dagger(F)|F\rangle, \\
&|F\alpha\bar{\beta}\rangle \equiv a_\alpha^\dagger(F)a_{\bar{\beta}}^\dagger(F)|F\rangle, \qquad |F\beta\bar{\alpha}\rangle \equiv \hat{\tau}|F\alpha\bar{\beta}\rangle = a_\beta^\dagger(F)a_{\bar{\alpha}}^\dagger(F)|F\rangle, \\
&|F\alpha\bar{\alpha}\rangle \equiv a_\alpha^\dagger(F)a_{\bar{\alpha}}^\dagger(F)|F\rangle, \qquad \text{with } \alpha<\beta \text{ and } 0<m_\alpha, m_\beta,
\end{aligned} \tag{54}$$

where m_α is the angular momentum z-component of state α. Time-reversed states are considered explicitly. The configurations of the type $|F\alpha\bar{\alpha}\rangle$ are like the vacuum invariant under time-reversal. The total MONSTER space contains as configurations $|q\rangle$ the set (54) and the vacuum

$$\{|q\rangle\} = \{|F\alpha\beta\rangle, |F\bar{\alpha}\bar{\beta}\rangle, |F\alpha\bar{\beta}\rangle, |F\beta\bar{\alpha}\rangle, |F\alpha\bar{\alpha}\rangle, |F\rangle;\ \alpha<\beta,\ 0<m_\alpha, m_\beta\}. \tag{55}$$

Out of these configurations we construct linear combinations which are either even or odd under time-reversal

$$|F\alpha\beta; SM_O^e\rangle \equiv \frac{1}{\sqrt{2}}\left[\hat{\Theta}_{MK_{\alpha\beta}}^S|F\alpha\beta\rangle \stackrel{+}{-} \pi_S(-)^{I_S-K_{\alpha\beta}}\hat{\Theta}_{M-K_{\alpha\beta}}^S|F\bar{\alpha}\bar{\beta}\rangle\right], \tag{56}$$

$$|F\alpha\bar{\beta}; SM_O^e\rangle \equiv \frac{1}{\sqrt{2}}\left[\hat{\Theta}_{MK_{\alpha\bar{\beta}}}^S|F\alpha\bar{\beta}\rangle \stackrel{+}{-} \pi_S(-)^{I_S-K_{\alpha\bar{\beta}}}\hat{\Theta}_{M-K_{\alpha\bar{\beta}}}^S|F\beta\bar{\alpha}\rangle\right], \tag{57}$$

where $K_{\alpha\beta} \equiv m_\alpha + m_\beta$ and $K_{\alpha\bar{\beta}} \equiv m_\alpha - m_\beta$. The projected states of type $|F\alpha\bar{\alpha}\rangle$ are either even or odd depending on the spin-parity of the considered symmetry S. For natural spin-parity, i.e. $\pi_S(-)^{I_S} = +1$, they are even, for unnatural spin-parity, i.e. $\pi_S(-)^{I_S} = -1$, they are odd :

$$|F\alpha\bar{\alpha}; SMe/o\rangle \equiv \frac{1}{2}\left[1 +/- \pi_S(-)^{I_S}\right]\hat{\Theta}_{M0}^S|F\alpha\bar{\alpha}\rangle. \tag{58}$$

The same holds for the symmetry-projected vacuum $|F;SM\rangle$. In shorthand notation we have

$$\{|\mathcal{Q};SMe\rangle,|\mathcal{Q};SMo\rangle\}\equiv\left\{\begin{array}{c}|F\alpha\beta;SMe\rangle,|F\alpha\beta;SMo\rangle,|F\alpha\bar{\beta};SMe\rangle,\\ |F\alpha\bar{\beta};SMo\rangle,|F\alpha\bar{\alpha};SMe/o\rangle,|F;SMe/o\rangle\end{array}\right\}. \tag{59}$$

The most general wave function in this space is then given by

$$\begin{aligned}|\psi_i(F);SM\rangle &= \sum_{\mathcal{Q}}\left\{|\mathcal{Q};SMe\rangle g^{Se}_{\mathcal{Q};i}+|\mathcal{Q};SMo\rangle g^{So}_{\mathcal{Q};i}\right\} &(60)\\ &= |F;SMe/o\rangle g^{Se/o}_{0;i}+\sum_{\substack{\alpha\\(0<m_\alpha)}}|F\alpha\bar{\alpha};SMe/o\rangle g^{Se/o}_{\alpha\bar{\alpha};i}\\ &\quad+\sum_{\substack{\alpha<\beta\\(0<m_\alpha,m_\beta)}}\Big\{|F\alpha\beta;SMe\rangle g^{Se}_{\alpha\beta;i}+|F\alpha\bar{\beta};SMe\rangle g^{Se}_{\alpha\bar{\beta};i}\\ &\qquad+|F\alpha\beta;SMo\rangle g^{So}_{\alpha\beta;i}+|F\alpha\bar{\beta};SMo\rangle g^{So}_{\alpha\bar{\beta};i}\Big\}. &(61)\end{aligned}$$

The expansion coefficients are obtained by diagonalizing the Hamiltonian (or, in order to take care of the center of mass motion the modified Hamiltonian (31)) according to equations (24,25). For this purpose we order the basis states $|\mathcal{Q}\rangle$ in such a way that first all "even" and then all "odd" configurations are listed. In this case the hermitean Hamiltonian matrix gets the form

$$\left(\begin{array}{cc}H^{ee}&H^{eo}\\H^{oe}&H^{oo}\end{array}\right)=\left(\begin{array}{cc}\Re e\ H^{ee}&i\,\Im m\ H^{eo}\\-i\,\Im m\ H^{oe}&\Re e\ H^{oo}\end{array}\right), \tag{62}$$

i.e., the matrix elements between two "even" or two "odd" states become purely real, the mixed matrix elements purely imaginary. This is explicitly shown for the two-quasiparticle states in appendix (A). (62) can be easily brought into the form

$$\left(\begin{array}{cc}\mathbf{1}&0\\0&-i\,\mathbf{1}\end{array}\right)\left(\begin{array}{cc}\Re e\ H^{ee}&\Im m\ H^{eo}\\\Im m\ (H^{eo})^T&\Re e\ H^{oo}\end{array}\right)\left(\begin{array}{cc}\mathbf{1}&0\\0&i\,\mathbf{1}\end{array}\right), \tag{63}$$

which demonstrates that only a real matrix has to be diagonalized in order to obtain the mixing coefficients g. For the construction of H^{ee}, H^{oo} and H^{eo} it is sufficient to calculate the matrix elements

$$\begin{array}{l}\langle\mathcal{Q}';SMe|\hat{H}|\mathcal{Q};SMe\rangle,\\ \langle\mathcal{Q}';SMo|\hat{H}|\mathcal{Q};SMo\rangle,\\ \langle\mathcal{Q}';SMe|\hat{H}|\mathcal{Q};SMo\rangle.\end{array} \tag{64}$$

Since the configurations $|\mathcal{Q}\rangle$ are linear combinations of type (56,57,58), this in turn means that we have to calculate the Hamiltonian matrix elements in between symmetry-projected states of type (55). Using the explicit form of the symmetry

projector (33), these are given by

$$\begin{aligned}\langle q'|\hat{H}\hat{\Theta}^{S}_{K_{q'}K_q}|q\rangle &= \frac{2I+1}{2}\int_0^\pi d\vartheta \sin(\vartheta) d^I_{K_{q'}K_q}(\vartheta)\frac{1}{(2\pi)^2}\int_{-\pi}^{\pi}d\varphi\int_0^\pi d\chi \\ &\quad \frac{1}{2}\Big\{ w(\varphi,\chi)\langle q'|\hat{H}\hat{\tilde{R}}(\tilde{\Omega})|q\rangle \\ &\quad + \pi_S\, w(\varphi,\chi)\langle q'|\hat{H}\hat{\tilde{R}}(\tilde{\Omega})\hat{\Pi}|q\rangle \\ &\quad + w(-\varphi,-\chi)\langle q'|\hat{H}\hat{\tilde{R}}(\vartheta,-\varphi,-\chi)|q\rangle \\ &\quad + \pi_S\, w(-\varphi,-\chi)\langle q'|\hat{H}\hat{\tilde{R}}(\vartheta,-\varphi,-\chi)\hat{\Pi}|q\rangle\Big\}. \end{aligned} \tag{65}$$

For the overlap matrices one gets the analogous equations just replacing the Hamilton operator by the unity operator **1**. Thus finally we are left with the problem to evaluate the rotated Hamiltonian matrix elements appearing in equation (65) and the corresponding rotated overlaps. The matrix elements which have the vacuum on both sides are just the rotated energy (47,49) and the rotated overlap (37). In addition there occur rotated matrix elements which have on one side the vacuum and on the other a two-quasiparticle state and rotated matrix elements in between two-quasiparticle states. A straightforward calculation yields for the former

$$\begin{aligned}&\langle F^1|\hat{H}\hat{\tilde{R}}(\tilde{\Omega})a^\dagger_\alpha(F^2_\lambda)a^\dagger_\beta(F^2_\lambda)|F^2_\lambda\rangle = \\ &\qquad n^{12}_\lambda(\tilde{\Omega})\left\{h^{12}_\lambda(\tilde{\Omega})[\tilde{g}^{12}_\lambda(\tilde{\Omega})]_{\alpha\beta} + [h^{02}_\lambda(F^1F^2;\tilde{\Omega})]_{\alpha\beta}\right\}\end{aligned} \tag{66}$$

with

$$[h^{02}_\lambda(F^1F^2;\tilde{\Omega})]_{\alpha\beta} \equiv \Big[X^{12^T}_\lambda(\tilde{\Omega})\Big(2H^{20^*}(F^1) + 12\tilde{H}^{40*}_\lambda(F^1F^2;\tilde{\Omega})\Big)X^{12}_\lambda(\tilde{\Omega})\Big]_{\alpha\beta}, \tag{67}$$

and

$$\begin{aligned}&\langle F^1|a_\beta(F^1)a_\alpha(F^1)\hat{H}\hat{\tilde{R}}(\tilde{\Omega})|F^2_\lambda\rangle = \\ &\qquad n^{12}_\lambda(\tilde{\Omega})\left\{h^{12}_\lambda(\tilde{\Omega})[g^{12}_\lambda(\tilde{\Omega})]_{\alpha\beta} + [h^{20}_\lambda(F^1F^2;\tilde{\Omega})]_{\alpha\beta}\right\}\end{aligned} \tag{68}$$

with

$$\begin{aligned}&[h^{20}_\lambda(F^1F^2;\tilde{\Omega})]_{\alpha\beta} \equiv \\ &\quad \Big[2H^{20}(F^1) + 2\tilde{H}^{22}(F^1F^2;\tilde{\Omega}) \\ &\qquad + \Big(H^{11}(F^1) - 3\tilde{H}^{31*}(F^1F^2;\tilde{\Omega})\Big)g^{12}_\lambda(\tilde{\Omega}) \\ &\qquad - \Big(\Big(H^{11}(F^1) - 3\tilde{H}^{31*}(F^1F^2;\tilde{\Omega})\Big)g^{12}_\lambda(\tilde{\Omega})\Big)^T \\ &\qquad + g^{12}_\lambda(\tilde{\Omega})\Big(2H^{20^*}(F^1) + 12\tilde{H}^{40*}(F^1F^2;\tilde{\Omega})\Big)g^{12}_\lambda(\tilde{\Omega})\Big]_{\alpha\beta},\end{aligned} \tag{69}$$

where

$$[\tilde{H}^{22}_{\lambda}(F^1F^2;\tilde{\Omega})]_{\alpha\beta} \equiv \sum_{\gamma\delta} H^{22}_{\alpha\beta\gamma\delta}(F^1)[g^{12}_{\lambda}(\tilde{\Omega})]_{\gamma\delta}, \tag{70}$$

$$[\tilde{H}^{31*}_{\lambda}(F^1F^2;\tilde{\Omega})]_{\alpha\beta} \equiv \sum_{\gamma\delta} H^{31^*}_{\alpha\beta\gamma\delta}(F^1)[g^{12}_{\lambda}(\tilde{\Omega})]_{\gamma\delta}, \tag{71}$$

and H^{11}, H^{20}, H^{22}, H^{31} and H^{40} being the matrix elements of the Hamiltonian (3) in the quasiparticle representation. The corresponding rotated overlaps are just the elementary contractions (41) and (39).

The rotated Hamiltonian matrix elements in between two-quasiparticle states on both sides are given by

$$\begin{aligned}
&\langle F^1|a_\beta(F^1)a_\alpha(F^1)\hat{H}\hat{\tilde{R}}(\tilde{\Omega})a^\dagger_\gamma(F^2)a^\dagger_\delta(F^2)|F^2_\lambda\rangle = \\
&\Big\{\Big([g^{12}_{\lambda}(\tilde{\Omega})]_{\alpha\beta}[\tilde{g}^{12}_{\lambda}(\tilde{\Omega})]_{\gamma\delta} + [X^{12}_{\lambda}(\tilde{\Omega})]_{\alpha\gamma}[X^{12}_{\lambda}(\tilde{\Omega})]_{\beta\delta} \\
&\quad - [X^{12}_{\lambda}(\tilde{\Omega})]_{\alpha\delta}[X^{12}_{\lambda}(\tilde{\Omega})]_{\beta\gamma}\Big)h^{12}_{\lambda}(\tilde{\Omega}) \\
&\quad + [g^{12}_{\lambda}(\tilde{\Omega})]_{\alpha\beta}[h^{02}_{\lambda}(F^1F^2;\tilde{\Omega})]_{\gamma\delta} + [\tilde{g}^{12}_{\lambda}(\tilde{\Omega})]_{\gamma\delta}[h^{20}_{\lambda}(F^1F^2;\tilde{\Omega})]_{\alpha\beta} \\
&\quad + [X^{12}_{\lambda}(\tilde{\Omega})]_{\alpha\gamma}[h^{11}_{\lambda}(F^1F^2;\tilde{\Omega})]_{\beta\delta} + [X^{12}_{\lambda}(\tilde{\Omega})]_{\beta\delta}[h^{11}_{\lambda}(F^1F^2;\tilde{\Omega})]_{\alpha\gamma} \\
&\quad - [X^{12}_{\lambda}(\tilde{\Omega})]_{\alpha\delta}[h^{11}_{\lambda}(F^1F^2;\tilde{\Omega})]_{\beta\gamma} - [X^{12}_{\lambda}(\tilde{\Omega})]_{\beta\gamma}[h^{11}_{\lambda}(F^1F^2;\tilde{\Omega})]_{\alpha\delta} \\
&\quad + [v_\lambda(F^1F^2;\tilde{\Omega})]_{\alpha\beta\gamma\delta}\Big\}n^{12}_{\lambda}(\tilde{\Omega}),
\end{aligned} \tag{72}$$

where

$$\begin{aligned}
[h^{11}_{\lambda}(F^1F^2;\tilde{\Omega})]_{\alpha\beta} \equiv \Big[&\Big\{H^{11}(F^1) - 3\tilde{H}^{31*}(F^1F^2;\tilde{\Omega}) \\
&+ g^{12}_{\lambda}(\tilde{\Omega})\left(2H^{20^*}(F^1) + 12\tilde{H}^{40*}_{\lambda}(F^1F^2;\tilde{\Omega})\right)\Big\}X^{12}_{\lambda}(\tilde{\Omega})\Big]_{\alpha\beta},
\end{aligned} \tag{73}$$

and

$$\begin{aligned}
&[v_\lambda(F^1F^2;\tilde{\Omega})]_{\alpha\beta\gamma\delta} \equiv \\
&\sum_{\rho\sigma}\Big\{4H^{22}_{\alpha\beta\rho\sigma}(F^1) - \sum_{\mu\nu}[g^{12}_{\lambda}(\tilde{\Omega})]_{\alpha\mu}[g^{12}_{\lambda}(\tilde{\Omega})]_{\beta\nu}24H^{40^*}_{\mu\nu\rho\sigma}(F^1) \\
&\qquad + \sum_{\nu}\left([g^{12}_{\lambda}(\tilde{\Omega})]_{\beta\nu}6H^{31^*}_{\alpha\nu\rho\sigma}(F^1) - [g^{12}_{\lambda}(\tilde{\Omega})]_{\alpha\nu}6H^{31^*}_{\beta\nu\rho\sigma}(F^1)\right)\Big\} \\
&\qquad\qquad [X^{12}_{\lambda}(\tilde{\Omega})]_{\rho\gamma}[X^{12}_{\lambda}(\tilde{\Omega})]_{\sigma\delta}.
\end{aligned} \tag{74}$$

The corresponding matrix elements of the rotated overlap are obtained as

$$\langle F^1|a_\beta(F^1)a_\alpha(F^1)\hat{\tilde{R}}(\tilde{\Omega})a^\dagger_\gamma(F^2)a^\dagger_\delta(F^2)|F^2_\lambda\rangle =$$
$$\Big\{[g^{12}_\lambda(\tilde{\Omega})]_{\alpha\beta}[\tilde{g}^{12}_\lambda(\tilde{\Omega})]_{\gamma\delta}$$
$$+ [X^{12}_\lambda(\tilde{\Omega})]_{\alpha\gamma}[X^{12}_\lambda(\tilde{\Omega})]_{\beta\delta} - [X^{12}_\lambda(\tilde{\Omega})]_{\alpha\delta}[X^{12}_\lambda(\tilde{\Omega})]_{\beta\gamma}\Big\}n^{12}_\lambda(\tilde{\Omega}). \qquad (75)$$

Various expressions occuring in the equations (66, 68, 72, and 67, 69) display certain symmetries related to time-reversal. These are presented in appendix (B) and have been used in the numerical calculation in order to reduce the actual number of matrix elements to be calculated [26].

Because of time-reversal, the vacuum as well as the two-quasiparticle excitations with respect to it contain only components corresponding to even mass numbers. If odd mass systems are to be considered, the above configuration space is therefore not applicable. Instead here, as already in the much more restricted *real* MONSTER calculations, we choose as configuration space the one-quasiparticle excitations of an even mass vacuum

$$\{|q\rangle\} \equiv \{|F\alpha\rangle, |F\bar{\alpha}\rangle, 0<m_\alpha\}, \qquad (76)$$

where we have introduced the definitions

$$|F\alpha\rangle \equiv a^\dagger_\alpha(F)|F\rangle \quad \text{and} \quad |F\bar{\alpha}\rangle \equiv \hat{\tau}|F\alpha\rangle = a^\dagger_{\bar{\alpha}}(F)|F\rangle. \qquad (77)$$

The energy spectrum can now be calculated in complete analogy to the even mass case. First we construct states with a good symmetry S which are either even or odd under time-reversal. They have the form

$$|F\alpha; SM^e_o\rangle \equiv \frac{1}{\sqrt{2}}\left[\hat{\Theta}^S_{Mm_\alpha}|F\alpha\rangle \stackrel{+}{-} \pi_S(-)^{j_S-m_\alpha}\hat{\Theta}^S_{M-m_\alpha}|F\bar{\alpha}\rangle\right], \qquad (78)$$

where small letters have been used for the angular momentum j_S and the angular momentum z-component m_α to indicate the half integer nature of these quantum numbers in odd mass nuclei. Denoting these configurations again by

$$\{|\mathcal{Q}; SMe\rangle, |\mathcal{Q}; SMo\rangle\} = \{|F\alpha; SMe\rangle, |F\alpha; SMo\rangle\}, \qquad (79)$$

the most general wave function for the odd mass case takes just the same form as for the even mass systems (60). Again the diagonalization of the Hamiltonian is reduced to a real problem according to equations (62,63,64).

The Hamiltonian matrix elements in between the one-quasiparticle configurations $|q\rangle$ of type (76), are calculated as shown in (65). I as well as K_q and $K_{q'}$ of formula (65) have to be replaced by the corresponding half integers. The procedure for the overlap matrix elements is analogous. In the end one has to calculate the rotated matrix elements of (65) in betweeen the one-quasiparticle states (76). The rotated

Hamiltonian matrix elements are obtained as

$$\langle F^1|a_\alpha(F^1)\hat{H}\hat{\tilde{R}}(\tilde{\Omega})a^\dagger_\beta(F^2_\lambda)|F^2_\lambda\rangle = \\ n^{12}_\lambda(\tilde{\Omega})\left\{h^{12}_\lambda(\tilde{\Omega})[X^{12}_\lambda(\tilde{\Omega})]_{\alpha\beta} + [h^{11}_\lambda(F^1F^2;\tilde{\Omega})]_{\alpha\beta}\right\}, \tag{80}$$

while the rotated overlap matrix elements are simply given by the elementary contraction (40). The symmetries of these matrix elements are displayed in appendix (B). In general this *complex* MONSTER approach for the description of odd mass nuclei cannot be expected to have the same quality as *complex* MONSTER for even mass nuclei. Especially when the mean field properties change quite much with the mass number, it is a clear drawback that the one-quasiparticle states are built on a *complex* VAMPIR determinant of a neighbouring even mass nucleus. It should be stressed, however, that because of the much richer structure of the *complex* VAMPIR solutions, the resulting configuration spaces are considerably larger than in the *real* case and hence a better description than by the latter can be expected also for odd mass nuclei.

Finally, we would like to mention, that for any particular symmetry S in the following always only one vacuum $|F^1\rangle \equiv |F^2\rangle \equiv |F\rangle$ will be used. Nevertheless, for the sake of generality, all formulas in the present section have been given for the case of two different vacua on both sides of any matrix element.

3 Application to ^{20}Ne and ^{22}Ne

As a first test the above described *complex* MONSTER approach was applied to the even-even nuclei ^{20}Ne and ^{22}Ne using only the $1s0d$ shell as single particle basis $\mathcal{D}$. This rather small basis was chosen in order to enable the comparison with complete shell model configuration mixing calculations. The single particle energies $t\,(d\,5/2) = -4.15$ MeV, $t\,(s1/2) = -3.28$ MeV, and $t\,(d\,3/2) = +0.93$ MeV have been taken from experiment [27] for protons as well as neutrons. As effective two-body interaction the mass-dependent version of the Chung and Wildenthal force [28] ($\hat{V}(A) = \hat{V}(18) \times (18/A)^\alpha$) has been used, with the only difference that instead of $\alpha = 0.3$ we took $\alpha = 1/3$. This force has been adjusted by its authors to many experimental data in various *sd* nuclei and is generally accepted to be "the standard" force for that model space. The comparison of the *complex* MONSTER approach with the exact shell model calculation provides a severe test of its quality. In addition the results are compared with those of the more restricted *real* MONSTER approach.

Let us first turn our attention to ^{20}Ne. This nucleus has two active protons and two active neutrons in the *sd* shell. The complete shell model diagonalization results in 640 different states : 46 $I^\pi = 0^+$, 97 $I^\pi = 1^+$, 143 $I^\pi = 2^+$, 129 $I^\pi = 3^+$,

109 $I^\pi = 4^+$, 64 $I^\pi = 5^+$, 36 $I^\pi = 6^+$, 12 $I^\pi = 7^+$, and 4 $I^\pi = 8^+$ states. In Fig. 1 the spectrum is plotted up to excitation energies of 16 MeV. The *complex* MONSTER approach reproduces all the 640 states exactly. This result is even independent of the underlying HFB transformation, provided the latter is essentially complex and breaks all the symmetries except time-reversal and axiality. The configuration mixing degrees of freedom of the *complex* MONSTER approach are here sufficient to reproduce the complete shell model spectrum. This is understandable since the *complex* MONSTER configuration space (59) contains in the *sd* shell altogether 277 configurations, no matter which particular (even mass) nucleus is considered. More precisely, one has 66 configurations of type $|F\alpha\beta; SMe\rangle$ and $|F\alpha\beta; SMo\rangle$ each, 66 of type $|F\alpha\bar{\beta}; SMe\rangle$ and $|F\alpha\bar{\beta}; SMo\rangle$ each, 12 of type $|F\alpha\bar{\alpha}; SMe/o\rangle$, and the projected vacuum $|F; SMe/o\rangle$. Out of these, 57 configurations can contribute to spin $I = 0$ states, 151 are available for $I = 1$ states, 223 for $I = 2$ states, 259 for $I = 3$ states, 275 for $I = 4$ states, and finally all 277 are available for each of the spin $I = 5, 6, 7, \ldots, 14$ states. Since the shell model spectrum is exactly reproduced, we can conclude that for ^{20}Ne this configuration space does contain all the shell model configurations.

The *complex* MONSTER approach is able to reproduce even those states, which cannot be described with the *complex* VAMPIR alone. These are states which contain the "missing couplings", mentioned in section (2.3), as irreducible substructures. In the case of ^{20}Ne, e.g., the lowest 3^+ and 5^+ shell model states belong to this category. Unfortunately there is no simple "geometrical" explanation for the "missing couplings". To identify them, one has to write each state in terms of two-particle couplings using the coefficients of fractional parentage. For bigger basis systems this becomes very difficult or even impossible. For four nucleons in the *sd* shell, however, this can be done easily : out of all 29 $(d5/2)^4$ configurations just two are inaccessible by the *complex* VAMPIR : the $[I^\pi = 3^+]_{T=0}$ and the $[I^\pi = 5^+]_{T=0}$ with maximal seniority, both being the dominant structures in the corresponding yrast states (see also [15]). These states are exactly reproduced by the *complex* MONSTER calculation. This is an example which shows that couplings, which are missing in the *complex* VAMPIR approach, can be accounted for by the configuration mixing of a subsequent *complex* MONSTER calculation. However, we would like to stress "missing couplings" do only occur because of the restriction to an axially and time-reversal symmetric HFB transformation. Using a HFB transformation without symmetry restrictions this problem is removed in the VAMPIR approach, too.

For comparison Fig. 1 also displays the spectrum obtained by the *real* MONSTER approach built on the mean field resulting from a *real* VAMPIR calculation for the 0^+ ground state : F(0^+). In the real case the MONSTER approach has much less degrees of freedom than in the complex case, and the MONSTER spectrum depends on the choice of the VAMPIR determinant [12]. First, a *real* VAMPIR calculation

in *sd* shell accounts only for 20 variational degrees of freedom, corresponding to the number of independent HFB transformation coefficients, while the *complex* VAMPIR has 56, i.e. almost a factor of three more degrees of freedom. Second, in a *real* MONSTER calculation there are altogether only 73 configurations available : the vacuum $|F;SM\rangle$, 12 configurations of type $|F\alpha\bar{\alpha};SM\rangle$, and 30 of type $|F\alpha\beta;SM\rangle$ and $|F\alpha\bar{\beta};SM\rangle$ each. 21 of these configurations can contribute to $I=0$ states, 30 to $I=1$ states, 61 to $I=2$ states, 56 to $I=3$ states, always 60 to the $I=5,7,9,11,13$ states, and always 73 to the $I=4,6,8,10,12,14$ states. These are only about one fourth of those available in the *complex* MONSTER approach. Therefore it is to be expected that the energies in ^{20}Ne obtained with the *real* MONSTER approach are higher than the exact ones, which are reproduced by the *complex* MONSTER calculation. It can be seen, however, that the difference in energy is small. On average one has for the yrast states a deviation of ~ 374 keV, i.e. ~ 0.9 % compared to the total energy of the shell model ground state, which is -41.412 MeV. The largest deviation, 624 keV, occurs for the $I^+=5^+$ state, the smallest for $I^+=6^+$ and amounts to 135 keV.

Finally we want to emphasize that the exact reproduction of the shell model spectrum of ^{20} Ne by the *complex* MONSTER approach is a very stringent non-trivial test of the computer code.

As second example ^{22}Ne was studied. For this nucleus there are in total 4206 shell model configurations : 216 $I^\pi=0^+$, 534 $I^\pi=1^+$, 777 $I^\pi=2^+$, 798 $I^\pi=3^+$, 723 $I^\pi=4^+$, 525 $I^\pi=5^+$, 345 $I^\pi=6^+$, 177 $I^\pi=7^+$, 81 $I^\pi=8^+$, 24 $I^\pi=9^+$, and 6 $I^\pi=10^+$ ones. In Fig. 2 for each spin only the lowest states resulting from the shell model diagonalization are plotted. The energies obtained by the *complex* and the *real* MONSTER approaches, respectively, are plotted up to 16 MeV excitation energy. For both MONSTER calculations the underlying HFB transformation was determined by a corresponding VAMPIR calculation for the 0^+ ground state. On average the *complex* MONSTER reproduces the shell model energies of ^{22}Ne rather well, but for most spin values not exactly, as it was the case in ^{20}Ne. Here, for the lower spin values $I^\pi=0^+,\ldots,7^+$ not all the above listed shell model configurations are contained in the MONSTER configuration space and only the states with angular momenta $I^\pi=8^+,\ldots,10^+$ are reproduced exactly. Small deviations are even found for the 7^+ states though the number of quasiparticle configurations is here larger than the correponding shell model dimension. This is due to the non orthogonality of the symmetry-projected determinants which in general causes some linear dependencies inbetween the various MONSTER configurations.

Again the *complex* MONSTER approach yields considerable improvements with respect to its *real* counterpart : the yrast states are more bound and many more of the excited shell model states can be described than in the latter case.

In Fig. 3 the energies of the yrast states in ^{22}Ne as obtained by various approaches are compared. The leftmost column shows the exact energies obtained by the complete shell model diagonalization. Then, from left to right, the energies calculated with the *complex* MONSTER, the *complex* VAMPIR, the *real* MONSTER, and the *real* VAMPIR are presented. Both MONSTER calculations have been based on the corresponding VAMPIR transformations obtained for the 0^+ ground state. Note that with the *real* VAMPIR approach only even spin states can be described. The average deviation of the energies obtained by the *complex* MONSTER approach from the shell model results is 103 keV. That is about 0.2 % of the shell model ground state energy of -58.820 MeV. The yrast states resulting from the *real* MONSTER approach display an average deviation of 539 keV from the exact results. This amounts to about 0.9 % of the shell model ground state energy.

Except for the 0^+ ground state, where, because of the stability of the *complex* VAMPIR solution with respect to arbitrary symmetry-projected two-quasiparticle excitations with $K = 0$, both methods yield identical results, and except for the 9^+ and 10^+ state, where the latter approach already reproduces the exact energies, the *complex* MONSTER solutions are more bound than the corresponding VAMPIR ones. This is essentially due to the admixture of configurations with $K \neq 0$. Furthermore it becomes obvious that the odd spin yrast states 1^+, 3^+, 5^+ and 7^+ are described rather poorly by *complex* VAMPIR alone. One can conclude that these states are again dominated by components corresponding to the above discussed "missing couplings". In fact, whenever the MONSTER result for an yrast state is considerably more bound than the correponding VAMPIR result this conclusion holds. This opens the possibility to identify "missing couplings" even in large model spaces where a decomposition of the configurations with the help of the coefficients of fractional parentage is not possible.

The even spin states obtained with the *real* VAMPIR approach are on average 360 keV less bound than the corresponding *complex* VAMPIR solutions. With the *real* MONSTER approach this average deviation is reduced to 98 keV. Exceptions are again the ground state, where MONSTER and VAMPIR solutions are again identical, and the 10^+ state, which is exactly reproduced by the *real* VAMPIR, while the MONSTER calculation yields 101 keV less energy. This indicates that configuration mixing on top of the real mean field determined for the 0^+ ground state is not suitable to describe this high spin excitation.

Finally we investigated the dependence of the *complex* MONSTER energies on the mean field determined by the preceeding *complex* VAMPIR calculation. For this purpose we have built always the full *complex* MONSTER spectrum on each of the yrast solutions obtained with the *complex* VAMPIR approach. The same was done in the *real* approximation. Obviously in this case only mean fields obtained for even spin states could be used.

As a typical example for the results of this investigation, Fig. 4 displays the dependence of the energies of the five lowest 0^+ states in ^{22}Ne on the spin-value used in the preceeding VAMPIR calculation. In addition, the leftmost column presents the energies of the three lowest shell model states. Solid lines denote the results of the *complex* MONSTER, dotted ones those of the *real* MONSTER approach. As can be seen, the *real* MONSTER results do depend only weekly on the underlying transformation. Here the differences in the various mean fields seem to be not very specific and can hence be compensated almost entirely by the configuration mixing. For the *complex* MONSTER results this does only hold as long as the 0^+, 2^+ or 4^+ VAMPIR transformations are taken. The higher even spin transformations, however, become now inadequate for the description of the 0^+ states. Thus one may conclude that the *complex* VAMPIR transformations display a much stronger dependence on the considered angular momentum than the more restricted *real* ones. As discussed above, due to "missing couplings", the odd spin yrast states are only poorly described by the *complex* VAMPIR approach. This is also reflected in the bad description of the 0^+ states, if the MONSTER diagonalization is based on an odd-spin transformation.

Similar dependencies on the underlying transformations as for the 0^+ states are obtained for other low spin values, too. Only for very high angular momenta where the *complex* MONSTER approach exhausts the complete shell model spaces the results become independent of the underlying transformation.

Finally, we would like to stress that in a MONSTER calculation (except for spin 0^+) the lowest yrast solution for a given angular momentum is not necessarily obtained using the VAMPIR transformation for this particular spin, but may result from a mean field derived for a neighbouring spin value. This was already found in *real* MONSTER calculations [12] and is due to the fact that mean field and configuration-mixing degrees of freedom are varied successively and not simultaneously.

4 Summary

In the last decade a couple of variational methods have been developed which have become known as the VAMPIR family. They all work with symmetry-projected HFB quasiparticle vacua as test wave functions, differ, however, in the degree of sophistication by which the underlying HFB transformations as well as the configuration mixing is determined. Originally, out of numerical reasons, in these methods only rather restricted HFB transformations were admitted : time-reversal invariance and axial symmetry were required, parity- and proton-neutron mixing were neglected and only *real* transformation coefficients were used. In the meantime most of these restrictions have been removed. Only the requirement of time-reversal and axiality

was kept and, e.g., essentially *complex* transformations were allowed. By these generalisation many more correlations are accounted for and the range of applicability of these few determinant approaches was considerably increased.

Unfortunately, by construction these methods are restricted to the lowest few states of a given symmetry only. Very often, however, one is interested in a complete set of particular excitations, e.g., those with respect to a specific transition operator. For such problems it is preferable to use a multi-configuration instead of a few determinant description. This is done in the MONSTER approach, which expands the nuclear wave function around the VAMPIR solution for the ground (or any other yrast) state and obtains the excitation spectrum by diagonalizing the chosen Hamiltonian in the space of the latter and all the symmetry-projected two-quasiparticle configurations with respect to it. Up to now such MONSTER calculations have only been done using the severly symmetry-restricted *real* HFB transformations mentioned above. In the present work, now the mathematical formalism as well as the numerical realisation of the MONSTER approach on the basis of the much more general *complex* HFB transformations has been developed.

With respect to the previous *real* implementation the *complex* MONSTER approach has a couple of essential advantages : first of all, the underlying HFB transformations account already for many more correlations than those used in the earlier calculations. Second, for the description of doubly odd systems one has not any more to rely on mean fields obtained for neighbouring doubly even nuclei but can use HFB transformations obtained for the particular system under consideration. Only for odd mass systems, which because of the even number parity of the underlying reference vacuum have still to be described by symmetry-projected one-quasiparticle states, one needs transformations from neighbouring nuclei. Third, the configuration spaces become considerably larger than in the more restricted *real* case and consequently a more complete and more detailed description of the nuclear spectra is to be expected. Last but not least, the admixture of two-quasiparticle configurations enables the description even of such states which are dominated by structures which are not contained in the symmetry-projected, time-reversal invariant HFB vacua used as test wave functions in the *complex* VAMPIR approach.

As a first test the *complex* MONSTER approach was applied to the nuclei ^{20}Ne and ^{22}Ne. For these calculations the $1s0d$ shell was chosen as basis. Thus the results could not only be compared with those of the more restricted *real* MONSTER approach but also with those of exact shell model diagonalizations, which are not available in larger model spaces. It was demonstrated that the complete shell model spectrum of ^{20}Ne is reproduced exactly by the *complex* MONSTER approach. For the heavier nucleus ^{22}Ne still an excellent approximation to the shell model spectrum is obtained. So, e.g., the average deviation of the energies of yrast states from the exact results amounts to only 0.2% of the shell model ground state energy. In both

nuclei the *complex* MONSTER approach yields considerable improvements with respect to the previous *real* MONSTER model. As compared to the above stated 0.2%, the real calculations give in both nuclei for the yrast energies an average deviation of 0.9%.

Already the *real* MONSTER approach was a rather useful tool for nuclear structure studies. It has been successfully applied to light as well as medium heavy nuclei. So, e.g., a rather nice description of various nuclei in the mass 130 region was obtained ([29], [30]). Since the *complex* MONSTER takes many additional correlations into account, we expect that this approach will develop into an even more powerful instrument for nuclear structure investigations in large model spaces.

Finally, we would like to stress that even in the *complex* MONSTER approach presented here, the underlying HFB transformations are still symmetry-restricted. Only if the additional violation of time-reversal invariance and axial symmetry is admitted, really optimal symmetry-projected vacua could be obtained by the VAMPIR variational procedure. In this case many additional correlations would be considered already on the mean field level. So, e.g., an unrestricted VAMPIR calculation in an $1s0d$-basis has 552 independent variational degrees of freedom as compared to the 56 ones present in the *complex* VAMPIR mean fields. As a consequence, obviously also the corresponding MONSTER configuration spaces are considerably increased and an even more detailed description of nuclear states can be expected. Unrestricted calculations along these lines are planned for the future.

We thank Prof. Dr. H. Müther for performing the shell model calculations. This work was partly supported by the Graduiertenkolleg "Struktur und Wechselwirkung von Hadronen und Kernen" (DFG, Mu 705/3).

Appendix

A Matrix elements in the "e/o" basis

In this section it is shown that in the "even-odd" basis because of its special properties under time-reversal only either purely real or purely imaginary matrix elements are obtained. As example the matrix elements of the Hamiltonian in between different two-quasiparticle configurations are presented.

$$
\begin{aligned}
&\langle F\alpha\beta;SMe|\hat{H}|F\gamma\delta;SMe\rangle \\
&= \frac{1}{2}\Big\{\langle F\alpha\beta|\hat{\Theta}^S_{K_{\alpha\beta}M}\hat{H}\hat{\Theta}^S_{MK_{\gamma\delta}}|F\gamma\delta\rangle \\
&\qquad + (-1)^{K_{\alpha\beta}-K_{\gamma\delta}}\langle F\bar{\alpha}\bar{\beta}|\hat{\Theta}^S_{-K_{\alpha\beta}M}\hat{H}\hat{\Theta}^S_{M-K_{\gamma\delta}}|F\bar{\gamma}\bar{\delta}\rangle \\
&\quad + \pi_S(-1)^{I_S-K_{\gamma\delta}}\Big[\langle F\alpha\beta|\hat{\Theta}^S_{K_{\alpha\beta}M}\hat{H}\hat{\Theta}^S_{M-K_{\gamma\delta}}|F\bar{\gamma}\bar{\delta}\rangle \\
&\qquad + (-1)^{K_{\alpha\beta}-K_{\gamma\delta}}\langle F\bar{\alpha}\bar{\beta}|\hat{\Theta}^S_{-K_{\alpha\beta}M}\hat{H}\hat{\Theta}^S_{MK_{\gamma\delta}}|F\gamma\delta\rangle\Big]\Big\} \\
&= \frac{1}{2}\Big\{\langle F\alpha\beta|\hat{\Theta}^S_{K_{\alpha\beta}M}\hat{H}\hat{\Theta}^S_{MK_{\gamma\delta}}|F\gamma\delta\rangle \\
&\qquad + \langle F\alpha\beta|\hat{\Theta}^S_{K_{\alpha\beta}M}\hat{H}\hat{\Theta}^S_{MK_{\gamma\delta}}|F\gamma\delta\rangle^* \\
&\quad + \pi_S(-1)^{I_S-K_{\gamma\delta}}\Big[\langle F\alpha\beta|\hat{\Theta}^S_{K_{\alpha\beta}M}\hat{H}\hat{\Theta}^S_{M-K_{\gamma\delta}}|F\bar{\gamma}\bar{\delta}\rangle \\
&\qquad + \langle F\alpha\beta|\hat{\Theta}^S_{K_{\alpha\beta}M}\hat{H}\hat{\Theta}^S_{M-K_{\gamma\delta}}|F\bar{\gamma}\bar{\delta}\rangle^*\Big]\Big\} \\
&= \Re e\ \langle F\alpha\beta|\hat{\Theta}^S_{K_{\alpha\beta}M}\hat{H}\hat{\Theta}^S_{MK_{\gamma\delta}}|F\gamma\delta\rangle \\
&\qquad + \pi_S(-1)^{I_S-K_{\gamma\delta}}\ \Re e\ \langle F\alpha\beta|\hat{\Theta}^S_{K_{\alpha\beta}M}\hat{H}\hat{\Theta}^S_{M-K_{\gamma\delta}}|F\bar{\gamma}\bar{\delta}\rangle. \qquad (81)
\end{aligned}
$$

In the same way one obtains

$$
\begin{aligned}
&\langle F\alpha\beta;SMo|\hat{H}|F\gamma\delta;SMo\rangle \\
&= \Re e\ \langle F\alpha\beta|\hat{\Theta}^S_{K_{\alpha\beta}M}\hat{H}\hat{\Theta}^S_{MK_{\gamma\delta}}|F\gamma\delta\rangle \\
&\qquad - \pi_S(-1)^{I_S-K_{\gamma\delta}}\ \Re e\ \langle F\alpha\beta|\hat{\Theta}^S_{K_{\alpha\beta}M}\hat{H}\hat{\Theta}^S_{M-K_{\gamma\delta}}|F\bar{\gamma}\bar{\delta}\rangle, \qquad (82)
\end{aligned}
$$

while for the mixed matrix elements one gets

$$
\begin{aligned}
&\langle F\alpha\beta;SMe|\hat{H}|F\gamma\delta;SMo\rangle \\
&= \frac{1}{2}\Big\{\langle F\alpha\beta|\hat{\Theta}^S_{K_{\alpha\beta}M}\hat{H}\hat{\Theta}^S_{MK_{\gamma\delta}}|F\gamma\delta\rangle \\
&\qquad - (-1)^{K_{\alpha\beta}-K_{\gamma\delta}}\langle F\bar{\alpha}\bar{\beta}|\hat{\Theta}^S_{-K_{\alpha\beta}M}\hat{H}\hat{\Theta}^S_{M-K_{\gamma\delta}}|F\bar{\gamma}\bar{\delta}\rangle \\
&\quad - \pi_S(-1)^{I_S-K_{\gamma\delta}}\Big[\langle F\alpha\beta|\hat{\Theta}^S_{K_{\alpha\beta}M}\hat{H}\hat{\Theta}^S_{M-K_{\gamma\delta}}|F\bar{\gamma}\bar{\delta}\rangle \\
&\qquad - (-1)^{K_{\alpha\beta}-K_{\gamma\delta}}\langle F\bar{\alpha}\bar{\beta}|\hat{\Theta}^S_{-K_{\alpha\beta}M}\hat{H}\hat{\Theta}^S_{MK_{\gamma\delta}}|F\gamma\delta\rangle\Big]\Big\} \\
&= i\ \Big\{\Im m\ \langle F\alpha\beta|\hat{\Theta}^S_{K_{\alpha\beta}M}\hat{H}\hat{\Theta}^S_{MK_{\gamma\delta}}|F\gamma\delta\rangle \\
&\qquad - \pi_S(-1)^{I_S-K_{\gamma\delta}}\ \Im m\ \langle F\alpha\beta|\hat{\Theta}^S_{K_{\alpha\beta}M}\hat{H}\hat{\Theta}^S_{M-K_{\gamma\delta}}|F\bar{\gamma}\bar{\delta}\rangle\Big\}, \qquad (83)
\end{aligned}
$$

and

$$
\begin{aligned}
&\langle F\alpha\beta;SMo|\hat{H}|F\gamma\delta;SMe\rangle \\
&= i\ \Big\{\Im m\ \langle F\alpha\beta|\hat{\Theta}^S_{K_{\alpha\beta}M}\hat{H}\hat{\Theta}^S_{MK_{\gamma\delta}}|F\gamma\delta\rangle \\
&\qquad + \pi_S(-1)^{I_S-K_{\gamma\delta}}\ \Im m\ \langle F\alpha\beta|\hat{\Theta}^S_{K_{\alpha\beta}M}\hat{H}\hat{\Theta}^S_{M-K_{\gamma\delta}}|F\bar{\gamma}\bar{\delta}\rangle\Big\}
\end{aligned}
$$

$$
\begin{aligned}
&= i \Big\{ - \Im m \, \langle F\gamma\delta|\hat{\Theta}^S_{K_{\gamma\delta}M}\hat{H}\hat{\Theta}^S_{MK_{\alpha\beta}}|F\alpha\beta\rangle \\
&\qquad + \pi_S(-1)^{I_S-K_{\alpha\beta}} \, \Im m \, \langle F\gamma\delta|\hat{\Theta}^S_{K_{\gamma\delta}M}\hat{H}\hat{\Theta}^S_{M-K_{\alpha\beta}}|F\bar{\alpha}\bar{\beta}\rangle \Big\} \\
&= \langle F\gamma\delta; SMe|\hat{H}|F\alpha\beta; SMo\rangle^*, \qquad (84)
\end{aligned}
$$

respectively.

B Symmetries

In this appendix some symmetry relations for matrix elements needed in *complex* MONSTER calculations are given. We restrict ourselves here to the Hamiltonian. For the overlap matrix elements similar expressions are valid.

For the rotated matrix elements of type

$$
[h_\lambda(F^1F^2;\vartheta,\varphi,\chi)]_{0\alpha\beta} \equiv \langle F^1|\hat{H}\hat{\tilde{R}}(\vartheta,\varphi,\chi)a^\dagger_\alpha(F^2)a^\dagger_\beta(F^2)|F^2_\lambda\rangle \qquad (85)
$$

one gets

$$
\begin{aligned}
[h_\lambda(F^1F^2;\vartheta,-\varphi,-\chi)]_{0\alpha\beta} &= [h_\lambda(F^1F^2;\vartheta,\varphi,\chi)]^*_{0\bar{\alpha}\bar{\beta}} \\
[h_\lambda(F^1F^2;\vartheta,-\varphi,-\chi)]_{0\alpha\bar{\beta}} &= -[h_\lambda(F^1F^2;\vartheta,\varphi,\chi)]^*_{0\bar{\alpha}\beta}, \qquad (86)
\end{aligned}
$$

while for the hermitean conjugate matrix elements

$$
[h_\lambda(F^1F^2;\vartheta,\varphi,\chi)]_{\alpha\beta0} \equiv \langle F^1|a_\beta(F^1)a_\alpha(F^1)\hat{H}\hat{\tilde{R}}(\vartheta,\varphi,\chi)|F^2_\lambda\rangle \qquad (87)
$$

one obtains

$$
\begin{aligned}
[h_\lambda(F^1F^2;\vartheta,-\varphi,-\chi)]_{\alpha\beta0} &= [h_\lambda(F^1F^2;\vartheta,\varphi,\chi)]^*_{\bar{\alpha}\bar{\beta}0} \\
[h_\lambda(F^1F^2;\vartheta,-\varphi,-\chi)]_{\alpha\bar{\beta}0} &= -[h_\lambda(F^1F^2;\vartheta,\varphi,\chi)]^*_{\bar{\alpha}\beta0}. \qquad (88)
\end{aligned}
$$

If the same vacuum is used on both sides, the above two types of matrix elements are connected via

$$
\begin{aligned}
[h_\lambda(F^1F^1;\vartheta,-\varphi,-\chi)]_{\alpha\beta0} &= (-1)^{K_{\alpha\beta}}[h_\lambda(F^1F^1;\vartheta,\varphi,\chi)]^*_{0\alpha\beta} \\
[h_\lambda(F^1F^1;\vartheta,-\varphi,-\chi)]_{\bar{\alpha}\bar{\beta}0} &= (-1)^{K_{\alpha\beta}}[h_\lambda(F^1F^1;\vartheta,\varphi,\chi)]^*_{0\bar{\alpha}\bar{\beta}} \\
[h_\lambda(F^1F^1;\vartheta,-\varphi,-\chi)]_{\alpha\bar{\beta}0} &= (-1)^{K_{\alpha\bar{\beta}}}[h_\lambda(F^1F^1;\vartheta,\varphi,\chi)]^*_{0\alpha\bar{\beta}} \\
[h_\lambda(F^1F^1;\vartheta,-\varphi,-\chi)]_{\bar{\alpha}\beta0} &= (-1)^{K_{\alpha\bar{\beta}}}[h_\lambda(F^1F^1;\vartheta,\varphi,\chi)]^*_{0\bar{\alpha}\beta}, \qquad (89)
\end{aligned}
$$

which yields for $[h^{02}_\lambda(F^1F^1;\tilde{\Omega})]_{\alpha\beta}$ and $[h^{20}_\lambda(F^1F^1;\tilde{\Omega})]_{\alpha\beta}$

$$
\begin{aligned}
[h^{02}_\lambda(F^1F^1;\vartheta,\varphi,\chi)]_{\alpha\beta} &= (-1)^{K_{\alpha\beta}}[h^{20}_\lambda(F^1F^1;\vartheta,\varphi,\chi)]_{\bar{\alpha}\bar{\beta}} \\
[h^{02}_\lambda(F^1F^1;\vartheta,\varphi,\chi)]_{\alpha\bar{\beta}} &= -(-1)^{K_{\alpha\bar{\beta}}}[h^{20}_\lambda(F^1F^1;\vartheta,\varphi,\chi)]_{\bar{\alpha}\beta}. \qquad (90)
\end{aligned}
$$

The same relations hold for $[\tilde{g}^{11}_{\lambda}(\tilde{\Omega})]_{\alpha\beta}$ and $[g^{11}_{\lambda}(\tilde{\Omega})]_{\alpha\beta}$.

For the rotated matrix elements

$$\begin{aligned}[h_\lambda(F^1F^2;\vartheta,\varphi,\chi)]_{\alpha\beta\gamma\delta} \equiv \\ \langle F^1|a_\beta(F^1)a_\alpha(F^1)\hat{H}\hat{\tilde{R}}(\vartheta,\varphi,\chi)a^\dagger_\gamma(F^2)a^\dagger_\delta(F^2)|F^2_\lambda\rangle \end{aligned} \tag{91}$$

we get

$$\begin{aligned}
[h_\lambda(F^1F^2;\vartheta,-\varphi,-\chi)]_{\alpha\beta\gamma\delta} &= [h_\lambda(F^1F^2;\vartheta,\varphi,\chi)]^*_{\bar{\alpha}\bar{\beta}\bar{\gamma}\bar{\delta}} \\
[h_\lambda(F^1F^2;\vartheta,-\varphi,-\chi)]_{\alpha\beta\bar{\gamma}\bar{\delta}} &= [h_\lambda(F^1F^2;\vartheta,\varphi,\chi)]^*_{\bar{\alpha}\bar{\beta}\gamma\delta} \\
[h_\lambda(F^1F^2;\vartheta,-\varphi,-\chi)]_{\alpha\beta\gamma\bar{\delta}} &= -[h_\lambda(F^1F^2;\vartheta,\varphi,\chi)]^*_{\bar{\alpha}\bar{\beta}\bar{\gamma}\delta} \\
[h_\lambda(F^1F^2;\vartheta,-\varphi,-\chi)]_{\alpha\beta\bar{\gamma}\delta} &= -[h_\lambda(F^1F^2;\vartheta,\varphi,\chi)]^*_{\bar{\alpha}\bar{\beta}\gamma\bar{\delta}} \\
[h_\lambda(F^1F^2;\vartheta,-\varphi,-\chi)]_{\alpha\bar{\beta}\gamma\delta} &= -[h_\lambda(F^1F^2;\vartheta,\varphi,\chi)]^*_{\bar{\alpha}\beta\bar{\gamma}\bar{\delta}} \\
[h_\lambda(F^1F^2;\vartheta,-\varphi,-\chi)]_{\alpha\bar{\beta}\bar{\gamma}\bar{\delta}} &= -[h_\lambda(F^1F^2;\vartheta,\varphi,\chi)]^*_{\bar{\alpha}\beta\gamma\delta} \\
[h_\lambda(F^1F^2;\vartheta,-\varphi,-\chi)]_{\alpha\bar{\beta}\gamma\bar{\delta}} &= [h_\lambda(F^1F^2;\vartheta,\varphi,\chi)]^*_{\bar{\alpha}\beta\bar{\gamma}\delta} \\
[h_\lambda(F^1F^2;\vartheta,-\varphi,-\chi)]_{\alpha\bar{\beta}\bar{\gamma}\delta} &= [h_\lambda(F^1F^2;\vartheta,\varphi,\chi)]^*_{\bar{\alpha}\beta\gamma\bar{\delta}}.
\end{aligned} \tag{92}$$

For identical vacua on both sides furthermore

$$[h_\lambda(F^1F^1;\vartheta,-\varphi,-\chi)]_{\alpha\beta\gamma\delta} = (-1)^{K_{\alpha\beta}+K_{\gamma\delta}}[h_\lambda(F^1F^1;\vartheta,\varphi,\chi)]^*_{\gamma\delta\alpha\beta} \tag{93}$$

holds.

Finally, for the Hamiltonian matrix elements in between two one-quasiparticle configurations

$$[h_\lambda(F^1F^2;\vartheta,\varphi,\chi)]_{\alpha\beta} \equiv \langle F^1|a_\alpha(F^1)\hat{H}\hat{\tilde{R}}(\vartheta,\varphi,\chi)a^\dagger_\beta(F^2)|F^2_\lambda\rangle \tag{94}$$

the relations

$$\begin{aligned}
[h_\lambda(F^1F^2;\vartheta,-\varphi,-\chi)]_{\alpha\beta} &= [h_\lambda(F^1F^2;\vartheta,\varphi,\chi)]^*_{\bar{\alpha}\bar{\beta}} \\
[h_\lambda(F^1F^2;\vartheta,-\varphi,-\chi)]_{\alpha\bar{\beta}} &= -[h_\lambda(F^1F^2;\vartheta,\varphi,\chi)]^*_{\bar{\alpha}\beta}
\end{aligned} \tag{95}$$

are found.

References

[1] R.R. Whitehead, A. Watt, B. J. Cole and I. Morrison, Adv. Nucl. Phys. **9** (1977) 123.

[2] P.J. Brussard and P.W.M. Glaudemans, "Shell Model Applications in Nuclear Spectroscopy", North-Holland, Amsterdam, 1977.

[3] J.B. McGrory, B.H. Wildenthal, Ann. Rev. Nucl. Part. Sci. **30** (1980) 383.

[4] K.W. Schmid and F. Grümmer, Rep. Prog. Phys. **50** (1987) 731.

[5] D.R. Hartree, Proc. Cambridge Philos. Soc. **24** (1928) 89.

[6] V. Fock, Z. Phys. **61** (1930) 126.

[7] N.N. Bogoliubov, Zk. Eksp. Teor. Fiz. **34** (1958) 58.

[8] N.N. Bogoliubov, Usp. Fiz. Nauk. **67** (1959) 541.

[9] N.N. Bogoliubov and V.G. Soloviev, Dokl. Akad. Nauk. SSSR **124** (1959) 1011.

[10] P. Ring and P. Schuck, "The Nuclear Many Body Problem", Springer, New York/Heidelberg/Berlin, 1980.

[11] K.W. Schmid, F. Grümmer and A. Faessler, Phys. Rev. C **29** (1984) 291.

[12] K.W. Schmid, F. Grümmer and A. Faessler, Nucl. Phys. **A431** (1984) 205.

[13] K.W. Schmid, F. Grümmer and A. Faessler, Ann. Phys. **180** (1987) 1.

[14] K.W. Schmid, F. Grümmer, M. Kyotoku and A. Faessler, Nucl. Phys. **A452** (1986) 493.

[15] K.W. Schmid, R.-R. Zheng, F. Grümmer and A. Faessler, Nucl. Phys. **A499** (1989) 63.

[16] A. Petrovici, K.W. Schmid, F. Grümmer and A. Faessler, Z. Phys. A **339** (1991) 71.

[17] K.W. Schmid, F. Grümmer and A. Faessler, Phys. Rev. C **29** (1984) 308.

[18] R.-R. Zheng, K.W. Schmid, F. Grümmer and A. Faessler, Nucl. Phys. **A494** (1989) 214.

[19] H.J. Mang, Phys. Rep. **18** (1975) 325.

[20] D.J. Thouless, Nucl. Phys. **21** (1960) 225.

[21] J.P. Elliott and T.H.R. Skyrme, Proc. R. Soc. London, Ser. A **323** (1955) 561.

[22] B. Giraud, Nucl. Phys. **71** (1965) 373.

[23] K.W. Schmid and R. Smith, Nucl. Phys. **A381** (1982) 195.

[24] N. Onishi and S. Yoshida, Nucl. Phys. **80** (1966) 367.

[25] K. Neergård and E. Wüst, Nucl. Phys. **A402** (1983) 311.

[26] E. Bender, PhD Thesis, in preparation.

[27] F. Ajzenberg-Selove, Nucl. Phys. **A460** (1986) 1.

[28] B.H. Wildenthal, Prog. Part. Nucl. Phys. **11** (1983) 5.

[29] E. Hammarén, K.W. Schmid, F. Grümmer, A. Faessler and B. Fladt, Nucl. Phys. **A437** (1985) 1.

[30] E. Hammarén, K.W. Schmid, F. Grümmer, A. Faessler and B. Fladt, Nucl. Phys. **A454** (1986) 301.

Figure Captions

Fig. 1 The energy spectrum for the nucleus ^{20}Ne as obtained by three different approaches : the complete shell model diagonalization (SCM, solid lines), the *complex* MONSTER (CM, dashed lines) and the *real* MONSTER (RM, dotted lines). The energy is given relative to the ^{16}O core. Only excitation energies up to 16 MeV above the shell model ground state are presented. The *real* MONSTER calculation has been based on the corresponding 0^+ VAMPIR transformation. The *complex* MONSTER results, which do reproduce all shell model states exactly, are independent of the particular choice of the underlying transformation.

Fig. 2 Same as Fig. 1, but for ^{22}Ne. For each spin only the lowest shell model states are presented. The *complex* MONSTER was here built on the *complex* VAMPIR solution obtained for the 0^+ ground state.

Fig. 3 The energies of the yrast states in ^{22}Ne as obtained by various approaches : the shell model (SCM), the *complex* MONSTER (CM) (again on top of the 0^+ VAMPIR solution), the *complex* VAMPIR (CV), the *real* MONSTER (RM) (based on the corresponding 0^+ VAMPIR solution, too), and the *real* VAMPIR (RV). In the last approach only the even spin states are accessible. Spin and parity are indicated on the l.h.s. of each level. Again the energy is given relative to the ^{16}O core.

Fig. 4 The five lowest 0^+ MONSTER states of ^{22}Ne are plotted versus the spin of the VAMPIR transformation which was used in each calculation. Solid lines refer to the *complex* MONSTER, dotted lines to the *real* MONSTER results. In the latter case only transformations with even spin values could be used. For comparison the lowest three 0^+ shell model (SCM) energies are also given. Again the energy is given relative to the ^{16}O core.

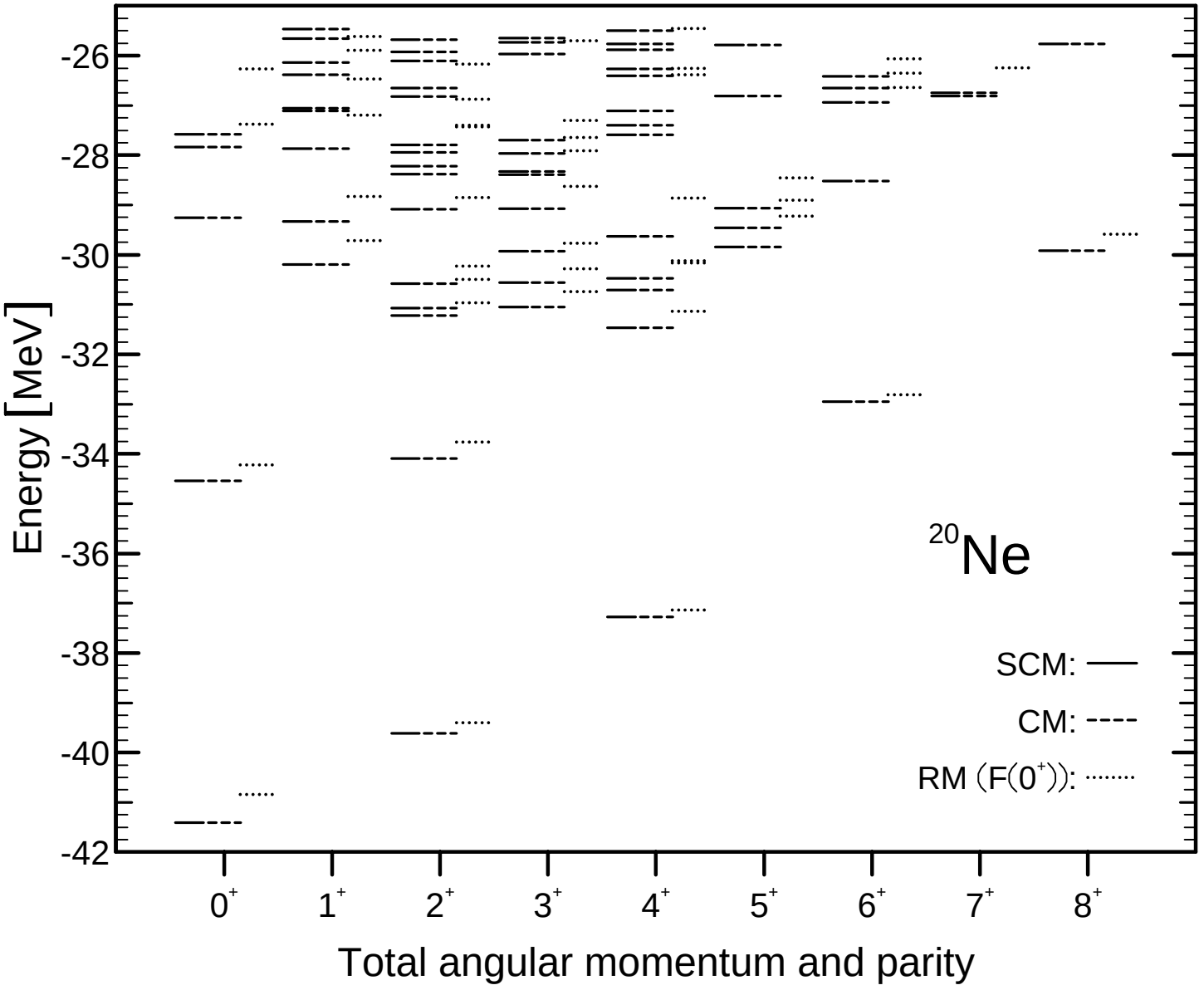
Energy [MeV]
-26
-28
-30
-32
-34
-36
-38
-40
-42
0+
1+
2+
3+
4+
5+
6+
7+
8+
Total angular momentum and parity
20Ne
SCM:
CM:
RM (F(0+)):

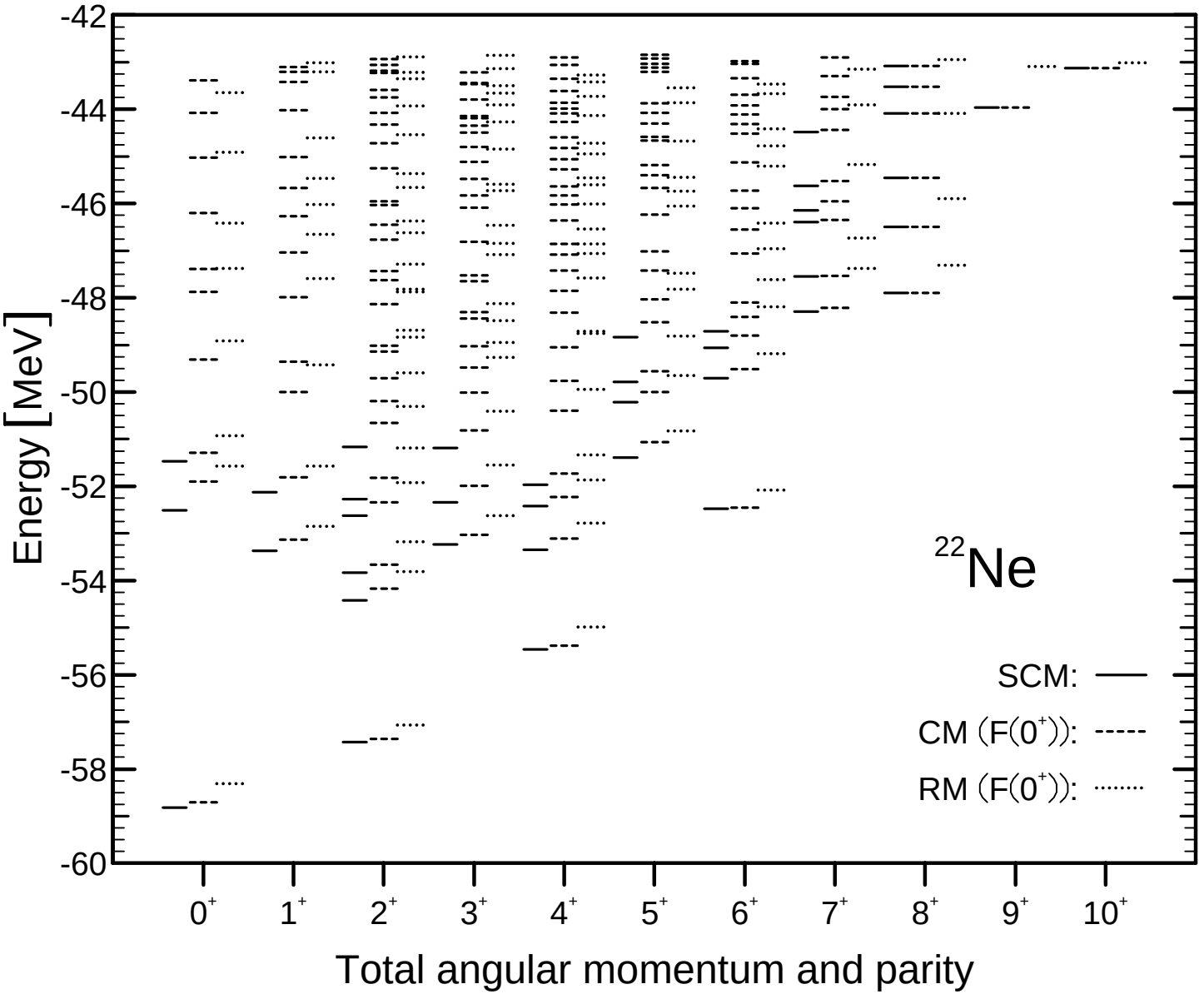
-42
-44
-46
-48
-50
-52
-54
-56
-58
-60
Energy [MeV]
^{22}Ne
SCM:
CM (F(0$^+$)):
RM (F(0$^+$)):
0$^+$
1$^+$
2$^+$
3$^+$
4$^+$
5$^+$
6$^+$
7$^+$
8$^+$
9$^+$
10$^+$
Total angular momentum and parity

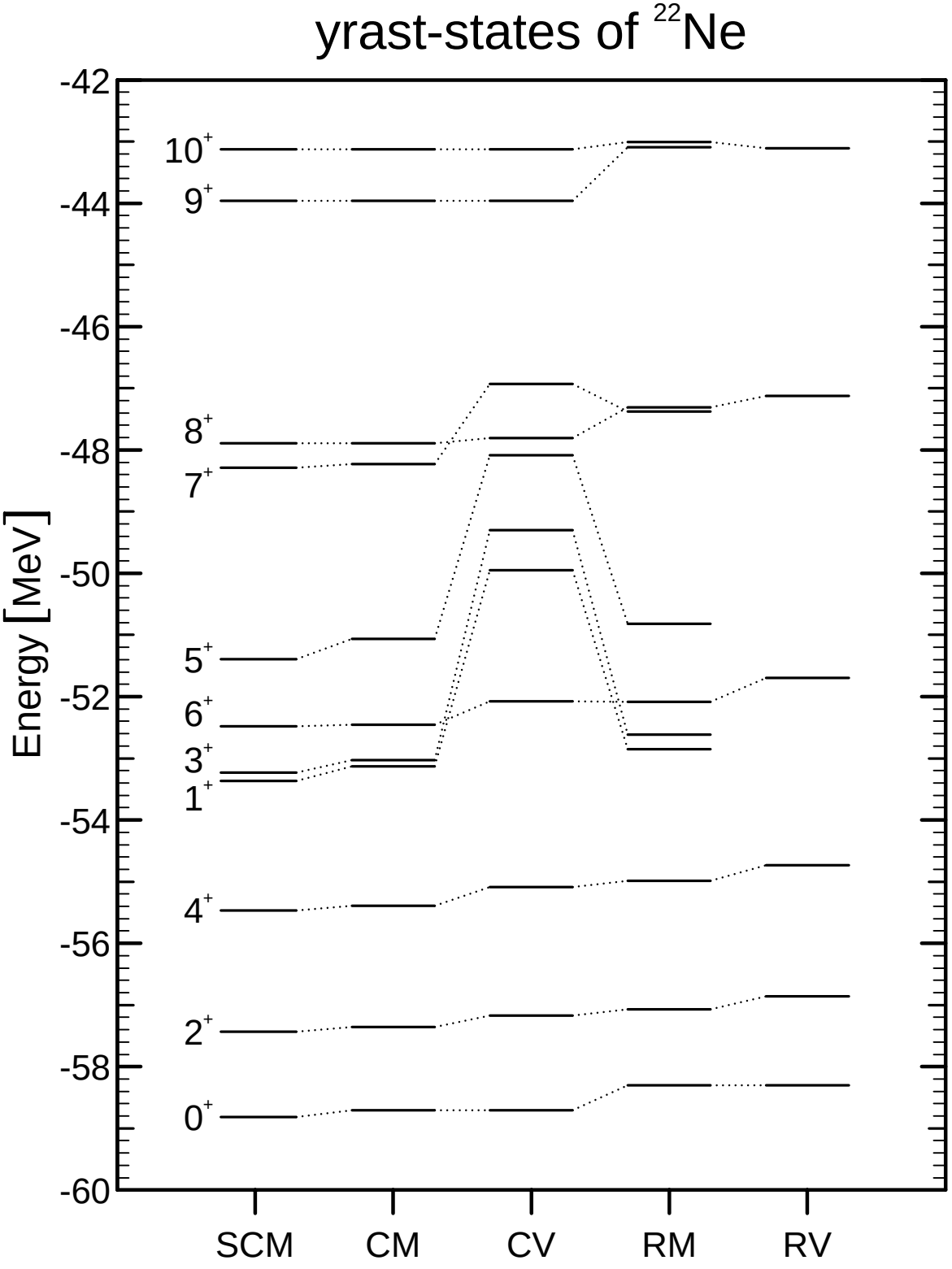
yrast-states of ^{22}Ne
Energy [MeV]
-42
-44
-46
-48
-50
-52
-54
-56
-58
-60
10^+
9^+
8^+
7^+
5^+
6^+
3^+
1^+
4^+
2^+
0^+
SCM
CM
CV
RM
RV

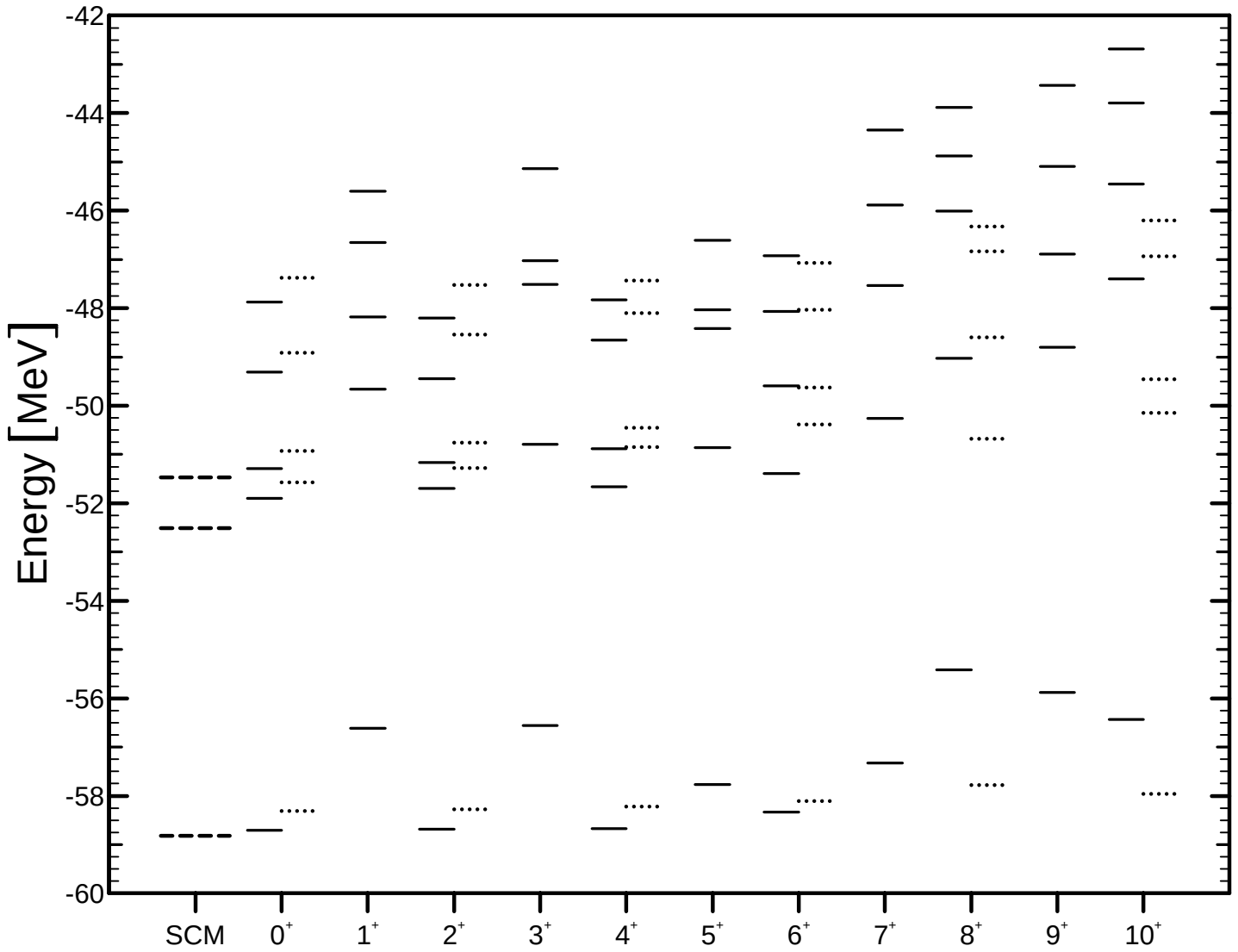
0+ states of 22Ne
Energy [MeV]
-42
-44
-46
-48
-50
-52
-54
-56
-58
-60
SCM
0+
1+
2+
3+
4+
5+
6+
7+
8+
9+
10+